Optimum Design of Steel Building Structures Using Migration-Based Vibrating Particles System

Siamak Talatahari [1, 2*], Shahin Jalili [3], Mahdi Azizi [1]

[1] Department of Civil Engineering, University of Tabriz, Tabriz, Iran.

[2] Engineering Faculty, Near East University, North Cyprus, Mersin 10, Turkey.

[3] School of Engineering, University of Aberdeen, King's College, Aberdeen, AB24 3UE, United Kingdom

Abstract

Vibrating Particles System (VPS) is developed based on some principles of physics in which the free vibration of a system with single degree of freedom including viscous damping is concerned. In this algorithm, each possible solution or vibrating particle seeks its equilibrium position in the search space. Despite of a relatively good exploration ability of the VPS algorithm, it is poor at exploitation and the convergence speed of this algorithm is also an issue in some cases. In this paper, the VPS algorithm is hybridized with the Migration-Based Local Search (MBLS) mechanism of the Biogeography-Based Optimization (BBO) algorithm with the strong local search capability to concentrate the search process around promising vibrating particles and locate the optimum solution more precisely. Three hybrid algorithms are developed based on how to use the VPS and MBLS methods as parallel, series and mixed series-parallel schemes. In order to evaluate the capability of the proposed hybrid methods in dealing with difficult structural optimization problems, a 24-story benchmark frame problem, a 10-story steel structure with 1026 structural members alongside a 20-story steel structure with 3860 members are optimized using presented algorithms. The findings affirm the robustness and efficiency of the proposed hybrid methods over the standard existing relevant approaches for optimum design of steel building structures.

Keywords: Optimum design; Steel structure; Vibrating particles system; Migration-based local search; Migration-based vibrating particles system.

* Corresponding author.
Email: siamak.talat@gmail.com
ORCID ID: https://orcid.org/0000-0002-1211-7148

1. Introduction

During the last decades, different optimization methods have been proposed/developed/applied and discussed by many researchers to utilize as metaheuristic techniques for optimum design of skeletal structures [1-4]. The fundamental goal of finding optimum designs of structures is the weight minimization of the structure considering the stress and deflection constraints required by the design codes and specifications. Among different optimization approaches presented in the literature, meta-heuristic approaches such as genetic algorithms (GAs) [5-7], Harmony Search (HS) algorithm [8,9], Ant Colony Optimization (ACO) [10,11], Imperialist Competitive Algorithm (ICA) [12, 13], and Bat Inspired (BI) algorithm [14,15] are the most common and efficient approaches, and they perform better than traditional methods in solving optimum structural problems. The advantages of using meta-heuristic algorithms for solving optimal design of structural problems are the optimum global solution finding procedure, powerful searching capability including simplicity, easily understood- main concept, easily usefulness, and higher rate of convergence.

The performance of the meta-heuristic algorithms mainly depends on the two major abilities, so-called exploration and exploitation. The exploitation ability ensures the solutions converge to the optimality, while exploration ability can provide an effective tool for avoiding local optimal solutions to explore the global regions of the search space more efficiently. So, providing a satisfactory balance between the exploitation and exploration abilities is a vital concern in utilizing and developing meta-heuristic algorithms for solving real-world optimization problems. Therefore, various hybrid and improved versions of optimization algorithms have been proposed by different researchers to provide new solutions to structural design problems. Exponential Big Bang-Big Crunch (EBB-BC) algorithm [16] for discrete design optimization of steel frames, Design-Driven HS (DDHS) algorithm [17] for steel frame optimization and Enhanced HS (EHS) algorithm [18] for optimum design of side sway steel frames are some examples of these hybrid and improved meta-heuristic methods, which were applied to solve frame design problems. Also, some other improved and hybrid metaheuristic approaches have been proposed in different engineering fields including the Chaos Game Optimization (CGO) [19] for engineering design purposes, Atomic Orbital Search (AOS) [20] for engineering optimization, Tribe-Interior Search Algorithm [21] for optimum design of building structures, quantum- behaved developed swarm optimizer [22] for optimal design of real- size building structures, Upper bound strategy for metaheuristic based design optimization of steel frames [23], computationally efficient optimum design of large scale steel

frames [24] and design optimization of real-size steel frames using monitored convergence curve [25].

The main aim of this paper is to develop a hybrid metaheuristic approach by utilizing the Vibrating Particles System (VPS) proposed by Kaveh and Ghazan [26] and the Biogeography-Based Optimization (BBO) algorithm developed by Simon [27]. In this regard, the VPS is determined as the main optimization algorithm while the Migration-Based Local Search (MBLS) mechanism of the BBO algorithm is inserted into the main algorithm in order to improve the capability of the VPS method in dealing with structural optimization problems. Three different hybrid approaches are developed based on the different configurations of the MBLS and VPS methods while in the proposed hybrid VPS-MBLS approaches, the VPS algorithm and the MBLS mechanism are hybridized with parallel, series and mixed series-parallel schemes. In order to evaluate the capability of the proposed hybrid methods in dealing with difficult optimization problems, a benchmark 24-story frame example as well as a 10-story steel structure with 1026 structural members alongside a 20-story structure with 3860 members are considered. In these structures, the design sections are selected as W-shaped sections for structural elements and the AISC-LRFD code [28] for steel structure design is utilized to determine the design requirements. The overall performance of the proposed hybrid methods is compared to the standard VPS and BBO algorithms.

Regarding the fact that hybrid metaheuristic algorithms are presented in this paper for optimum design of building structures, it should be noted that many other hybrid schemes have also been proposed in the literature in which the discrete structural optimization is in perspective. Hybrid plant growth simulation and particle swarm optimization algorithm for structural optimization [29], hybrid Water Cycle and Moth-Flame for solving constrained optimization problems in engineering field [30], Hybrid Harris hawks optimization, slap swarm algorithm, grasshopper optimization and dragonfly algorithm for design optimization of structures [31], hybrid particle swarm and gradient algorithm for structural design optimization [32], Hybrid harmony search, particle swarm and ant colony algorithm for design optimization of structures [33], hybrid Charged System Search-MBLS algorithm for optimum design of truss structures [34], hybrid scheme by implementation of migration and differential evolution strategies in optimization of truss structures [35], hybrid Simulated Annealing (SA), Harmony Search (HS) and Big Bang-Big Crunch (BBBC) for structural optimization [36], hybrid adaptive meshing strategy (AMS) and bidirectional evolutionary for structural optimization [37], and hybrid evolutionary algorithm for structural optimization [38].

The rest of the paper is organized as follows: the general formulation of the main optimization problem for optimum design of steel building structures is presented in Section 2. A brief review of VPS algorithm and MBLS mechanism of the BBO algorithm are discussed in Section 3. Section 4 presents detailed explanation of the proposed hybrid VPS-MBLS approaches. In section 5, the utilized design examples are presented in detail. Section 6 validates the performances of the proposed hybrid algorithms through comparing them against the standard VPS and BBO algorithms. Finally, the conclusions from the present study are drawn in Section 7.

2. Optimum Design of Steel Frames

2.1. Objective Function

The main purpose of structural optimization is to select suitable sections based on a set of predefined sections for structural members in order to satisfy the design constraints. In optimal design of steel structural frames, there is an assumption that N_m structural members are grouped into N_d design groups. In this regard, a vector of integer values is considered for determination of the sequence numbers in steel design sections assigned to N_d member groups in order to minimize the total weight of the structure. The integer vector and the overall weight of the considered structure is presented as follows:

$$\text{Find} \quad I^T = [I_1, I_2, \dots, I_{N_d}] \tag{1}$$

$$\text{To minimize} \quad W = \sum_{i=1}^{N_d} \rho_i . A_i \sum_{j=1}^{N_t} L_j \tag{2}$$

where, ρ_i and A_i are the unit weight and length of the steel design section determined for member group i, respectively; N_t is the total number of all structural members in group i and L_j is the length of the *jth* member belonging to the *ith* group.

2.2. Design Constraints

Based on the AISC-LRFD code [28] for steel structure design, two main design requirements are the strength and serviceability [39]. By trying find the minimum weight of structures, the following constraints must be fulfilled for the design sections' strength requirements:

$$C_{IEL}^i = \left[\frac{P_{uJ}}{\varphi P_n}\right]_{IEL} + \frac{8}{9}\left(\frac{M_{uxJ}}{\varphi_b M_{nx}} + \frac{M_{uyJ}}{\varphi_b M_{ny}}\right)_{IEL} - 1 \le 0 \quad for \quad \left[\frac{P_{uJ}}{\varphi P_n}\right]_{IEL} \ge 0.2 \tag{3}$$

$$C_{IEL}^{i} = \left[\frac{P_{uJ}}{2\varphi P_n}\right]_{IEL} + \left(\frac{M_{uxJ}}{\varphi_b M_{nx}} + \frac{M_{uyJ}}{\varphi_b M_{ny}}\right)_{IEL} - 1 \leq 0 \quad for \quad \left[\frac{P_{uJ}}{\varphi P_n}\right]_{IEL} < 0.2 \tag{4}$$

$$C_{IEL}^{v} = (V_{uJ})_{IEL} + (\varphi_v V_n)_{IEL} \leq 0 \tag{5}$$

where, IEL is the element number as $IEL = 1,2,\dots,NEL$ and NEL is the overall number of elements; J is the load combination number as $J = 1,2,\dots,N$ and N is the total number of all design load combinations; P_{uJ} is the required compressive or tensile (axial) strength, under Jth design load combination; M_{uxJ} and M_{uyJ} are the total flexural strengths required for bending of structural elements about x and y, under the Jth design load combination, respectively; where for strong and weak axes bending, the x and y subscripts utilized as the relating symbols, respectively. P_n, M_{nx} and M_{ny} are the nominal compressive or tensile (axial) and flexural (for bending of structural elements about x and y axes) strengths of the IELth member under consideration. φ is the axial strength's resistance factor formulated regarding to the yielding of the gross section (0.85 for compression and 0.9 for tension) and φ_b is the flexural resistance factor (0.9). V_{uJ} is the shear strength required under Jth design load combination and V_n is the nominal shear strength of the IELth considered member and φ_v is 0.9.

The nominal tensile strength of the members is related to the yielding of the gross section and calculated as follows:

$$P_n = F_y A_g \tag{6}$$

where, F_y is the specific yield stress of the structural members and A_g is the gross section of the structural members.

The nominal compressive strength of the members is calculated in a different way than the tensile one while it has smaller value and is calculated based on the limit states of torsional buckling, flexural buckling, and flexural–torsional buckling. The nominal compressive strength of the members based on the limit state of flexural buckling (with non-compact alongside compact elements), is as follows:

$$P_n = F_{cr} A_g \tag{7}$$

where F_{cr} is the critical stress relating to the flexural buckling of the member.

Based on the flange local buckling, limit states of yielding, lateral–torsional buckling, and web local buckling, the member's minimum nominal flexural strength is obtained. Regarding the limit state of yielding, the flexural capacity is as following:

$$M_n = M_p = ZF_y \leq 1.5SF_y \tag{8}$$

where Z is the modulus of plasticity and S is the member's section modulus about the axis of bending. The flexural capacity regarding to the limit state of buckling in lateral–torsional state for sections which are doubly symmetric, is as followings:

$$M_n = \begin{cases} M_p & if \;\; l_b \leq l_p \\ C_b\left[M_p - \left(M_p - M_r\right)\left(\dfrac{l_b - l_p}{l_r - l_p}\right)\right] \leq M_p & if \;\; l_p < l_b \leq l_r \\ M_{cr} \leq M_p & if \;\; l_b > l_r \end{cases} \tag{9}$$

$$C_b = \frac{12.5M_{max}}{2.5M_{max} + 3M_A + 4M_B + 3M_C} \tag{10}$$

where, l_b , l_p , l_r , M_r , M_{cr} , and C_b are the member's lateral unbraced length, the limiting lateral unbraced length relating to the full bending capacity in plastic state, the limiting lateral unbraced length for inelastic buckling of lateral–torsional, the limiting amount of buckling moment, the critical moment in elastic state for the buckling of lateral–torsional, and the modification factor representing a non-uniform moment diagram respectively. M_{max}, M_A, M_B, and M_C are the absolute values relating to maximum moment, moment at the quarter point, moment at the centerline, and moment at the three-quarter point of the unbraced segment, respectively.

For doubly symmetric members exposed to shear force in the plane of the web, the nominal shear strength of unstiffened webs is as followings:

$$V_n = 0.6F_{yw}A_w \qquad for \quad h/t_w \leq 418/\sqrt{F_{yw}} \tag{11}$$

$$V_n = 0.6F_{yw}A_w\,(418/\sqrt{F_{yw}})/(h/t_w) \qquad for \quad 418/\sqrt{F_{yw}} < h/t_w \leq 523/\sqrt{F_{yw}} \tag{12}$$

$$V_n = 132000\,A_w/(h/t_w)^2 \qquad for \quad 523/\sqrt{F_{yw}} < h/t_w \leq 260 \tag{13}$$

where, h represents the clear distance between flanges less the corner radius or fillet for rolled shapes; t_w is the total thickness of web; A_w is the area for shear and F_{yw} is the web's yield stress.

Beyond the strength requirements, some other criteria called serviceability requirements should be concerned in designing process as follows:

$$C_D^t = \Delta_{MaxJ} - \Delta_{Max}^a \leq 0 \tag{14}$$

$$C_F^d = \left[\delta_J\right]_F - [\delta^a]_F \leq 0 \tag{15}$$

A comparison between the maximum lateral displacement of the considered structure in the Dth direction for $D = 1,2,\dots,ND$ under Jth design load combination, (Δ_{MaxJ}) regarding the maximum allowable lateral displacement (Δ_{Max}^a) is provided by Eq. (14). The Eq. (15) compares the inter-story drift of the Fth story for $F = 1,2,\dots,NF$ (NF is the total number of stories) under the Jth design load combination $\left[\delta_J\right]_F$ against the related allowable value $[\delta^a]_F$.

3. Review on Utilized Optimization Methods

In this section, a brief review is provided for the standard Vibrating Particles System (VPS) algorithm and the Migration-Based Local Search (MBLS) mechanism of the Biogeography-Based Optimization (BBO) algorithm. It should be noted that all of the internal parameters in the utilized algorithms are derived of the latest literatures in which multiple parameter tuning processes were conducted in order to provide a proper range for these parameters.

3.1. Vibrating Particles System (VPS) Algorithm

Two types of vibration are known for a particle in the space as a free or forced vibrations. In the free vibration, there is not any externally induced action on the particle and the vibration of the particle is based on the initial conditions while for the forced vibration, a periodic force which is created based on an externally induced velocity or displacement is applied to the particle. In order to consider the vibration motion of a particle, a system of elements including a block of mass (m), a block of spring (k) and a block of viscous damping (c) are required in order to configure a system with single degree of freedom (Fig. 1).

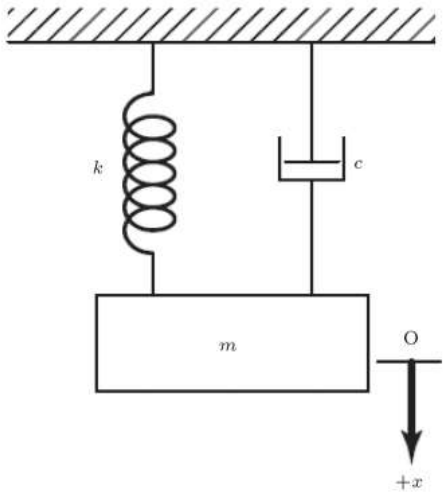

Fig. 1. Free vibration of a system with single degree of freedom including damping [26].

Considering the general configuration of a system including single degree of freedom, the equation which represent the vibrational motion of this system is determined as follows:

$$M\ddot{x} + C\dot{x} + Kx = 0 \tag{16}$$

where M is defined as the mass, K is defined as the stiffness and C is defined as the coefficient of viscos damping for the single degree of freedom system.

In order to have a solution for this equation, the natural frequency of the considered system (ω_n) and the critical damping coefficient (c_c) are defined as follows:

$$\omega_n = \sqrt{K/M} \tag{17}$$

$$C_c = 2M\omega_n \tag{18}$$

Based on some main principles in dynamics of structures, the mathematical solution of Eq. 1 for the under damped systems ($C < C_c$) is determined as follows:

$$x(t) = \rho e^{-\zeta\omega_n t}\sin(\omega_D t + \phi) \tag{19}$$

$$\omega_D = \omega_n \sqrt{1 - \zeta^2} \tag{20}$$

$$\zeta = c/2m\omega_n \tag{21}$$

where ρ and ϕ are two constant values which are determined based on the initial conditions of the system; ω_D is the damped frequency of the considered system; and ζ is the damping ratio. The vibrational motion of a system including single degree of freedom considering four types of different damping ratios are demonstrated in Fig. 2.

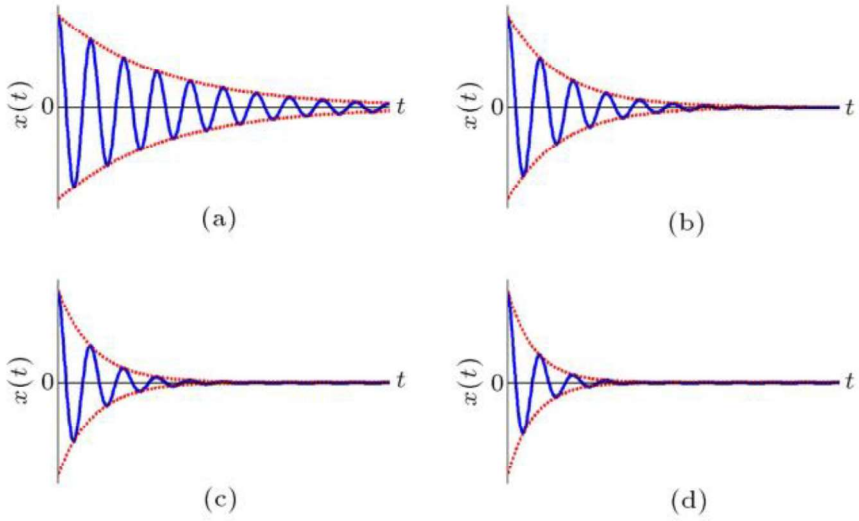

Fig. 2. Free vibration of a system with single degree of freedom considering four levels of damping ratio as (a) 5%, (b) 10%, (c) 15%, (d) 20% [26].

In the mathematical formulation of the VPS algorithm, the previously provided principles for the free vibration of a system with single degree of freedom are utilized which lead to a proper optimization algorithm. In the first step of the algorithm, the initialization process is conducted in which the initial values of the decision variables and the initial positions of the solution candidates or Vibrating Particles (VP) are all determined by the following equation:

$$x_i^j = x_{min} + rand.(x_{max} - x_{min}) \quad (22)$$

where x_i^j is the *jth* decision variable of the *ith* VP; x_{min} and x_{max} are the lower and upper bound of the variables and $rand$ is a uniformly distributed random number in the range of [0, 1].

In the next step, three different parameters are determined as *GB* representing a good vibrating particle, *BP* representing a bad vibrating particle, and *HB* as the best so far found vibrating particle between all of the particles. The *GB* and *BP* are determined randomly in each iteration between the best and the worst so far found solutions while *HB* is determined in each iteration and reported as the best solution of the optimization process. Another parameter (D) is also determined and updated in each iteration which controls the convergence of the algorithm which is presented as follows:

$$D = \left(\frac{iter}{iter_{max}}\right)^{-\alpha} \quad (23)$$

where α is a constant value (0.05 in this paper), $iter$ is the current iteration and $iter_{max}$ is the maximum number of iterations.

Based on the initialization, the position updating process for the VPs in the next generations are conducted by the following equations:

$$x_i^j = w_1.\left[D.A.rand_1 + HB^j\right] + w_2.\left[D.A.rand_2 + GP^j\right] + w_3.\left[D.A.rand_3 + BP^j\right] \quad (24)$$

$$A = [w_1.(HB^j - x_i^j)] + [w_2.(GP^j - x_i^j)] + [w_3.(BP^j - x_i^j)] \quad (25)$$

where $rand_1$, $rand_2$ and $rand_3$ are three randomly generated numbers which are distributed uniformly in the range of [0, 1]; w_1, w_2 and w_3 are three constant values which represent the importance of the HB, GP and BP in the position updating process.

In order to determine w_1, w_2 and w_3 in each iteration, another parameter (p) is considered. For a random number which is uniformly distributed in the range of [0, 1], if the random number is less than p, $w_3 = 0$, $w_2 = 1 - w_1$ are considered accordingly.

For the VPs which violates the boundary conditions, a side constraint handling process is formulated based on the well-known Harmony Search (HS) algorithm [9] in which the Harmony Memory Considering Rate (HMCR) is determined as 0.75 and the Pitch Adjusting Rate (PAR) is determined as 0.15.

3.2. Migration-Based Local Search (MBSL) Mechanism

Biogeography-based optimization (BBO) is one of the modern meta-heuristic algorithms designed by Simon [27] to find optimum solutions to the real-world engineering optimization problems. BBO is an algorithm formulated based on population which simulates the migration behavior of species while searching for suitable habitats. Each habitat represents a specific point in the considered search space, and hence a possible solution candidate to the optimization problem. In the n-dimensional search space, the suitability index variables (SIVs) are determined in order to represent the position of considered habitats and the solution quality is measured by the habitat suitability index (HSI). The HSI value for each habitat is directly proportional to the objective function value. Thus, a habitat with higher HSI value is a better solution for the problem. Based on the probabilistic mathematical models of the biogeography science [40], the habitats with the higher HSI values tend to absorb a larger number of possible species.

The BBO algorithm employs a migration operator to simulate migration procedure between different habitats. The considered migration operator shares information between the habitats based on the immigration λ_i and emigration μ_i rates. For each habitat in the considered search space, the two immigration λ_i and emigration μ_i rates are defined based one the migration model and HSI values. Different migration models exist which can be considered for calculating these

rates. A simple linear migration model is presented in Fig. 3 in which the immigration λ_i and emigration μ_i rates are linear functions of HSI values (or number of species). It is observed that the worse habitat (poor solution candidate with lower HSI value) like S_1 has a high immigration rate λ_i and a low emigration rate μ_i. In other words, such habitats modify their position by taking information of the other habitats with the high probability, while they share information among the other habitats with the relatively low probability. In addition, the habitat with more species (some good solution candidates with higher HIS value) like S_2 has a lower immigration rate λ_i with a higher emigration rate μ_i. Therefore, better habitats with higher HSI values tend to share their good information about the search space with a higher probability. Moreover, the habitat which has medium HIS value, such as point S_0, both immigration λ_i and emigration μ_i rates are equal. In addition, the probability of collecting information from the other habitats or even sharing its information among other habitats is equal. This point is called as equilibrium number of species. The migration procedure can be defined as follow:

$$\boldsymbol{X}_i(SIVs) \longleftarrow \boldsymbol{X}_j(SIVs) \tag{26}$$

where $\boldsymbol{X}_j$ and $\boldsymbol{X}_i$ are the emigrating and immigrating habitats, respectively. The considered habitats are selected probabilistically based on the emigration and immigration rates using a selection approach such as roulette wheel method. Considering the migration process of the BBO algorithm, one of the *SIVs* of the *i*th habitat is replaced by the *SIVs* of *j*th habitat. Figure 2 presents the migration process of the BBO algorithm.

4. Hybrid VPS-MBLS Approaches

In the meta-heuristic algorithms, the procedures of the exploitation and the exploration are different from each other and achieving adequate balance between them is a major issue in gaining good optimization performance. The VPS algorithm is an effective technique for solving different global optimization problems. However, VPS could have some problems with convergence issues and entrap in a local optimum solution. In addition, the MBLS mechanism with the strong local search capability is able to concentrate the searching process around successful candidate solutions in order to identify the optimum solution more precisely. In the proposed VPS-MBLS algorithms, the balance between exploitation and exploration is achieved using the VPS as a global optimization technique for global exploration and the MBLS as a strong local search mechanism for local exploitation. These algorithms effectively use the advantages of both the VPS algorithm and the MBLS approach and avoid their deficiencies.

To implement the migration process among the VPs in the considered search space, the immigration λ_i and emigration μ_i rates should be determined for each VP considering the objective function value and the migration model. Based on the simple linear model for the migration which is previously proposed, sum of the emigration (μ_i) and the immigration (λ_i) rates for each VP should be set to unity (Fig. 3).

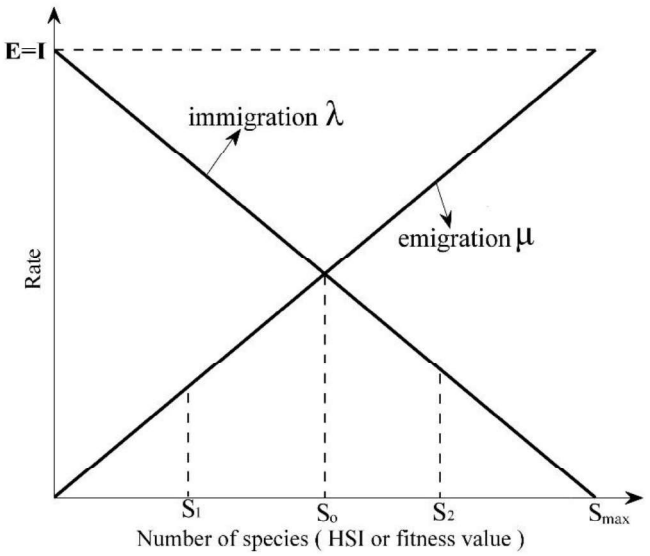

Fig. 3. The schematic presentation of the Simple linear migration model [27].

After calculating λ_i and μ_i rates for all VPs based on the HSI values or objective function values in each VP, the migration process occurs between two different VPs as follow:

$$\boldsymbol{X}_{ik} \longleftarrow \boldsymbol{X}_{jk} \tag{27}$$

where $\boldsymbol{X}_{jk}$ and $\boldsymbol{X}_{ik}$ are kth variable of the emigrating and the immigrating VPs, respectively. These VPs are selected probabilistically considering the emigration and the immigration rates as described previously.

Based on the type of the hybridization, the proposed three hybrid algorithms are described in the following subsections.

4.1. VPS-MBLS with parallel scheme (VPS-MBLS I)

In the first hybrid approach, the VPS algorithm has been hybridized with MBLS mechanism with parallel scheme as shown in Fig. 4. By considering the provided flowchart, the following points can be concluded:

- Two mechanisms are considered for position update of each VP in the considered search space determined as the VPS algorithm and the MBLS mechanism.

- A migration process is considered for each VP toward another VP in the considered search space with the probability of λ_i in order to exploit better solutions with the higher qualities around the VPs.
- Otherwise, each VP will be moved by standard VPS algorithm to provide efficient exploration of search space and mitigate premature convergence.

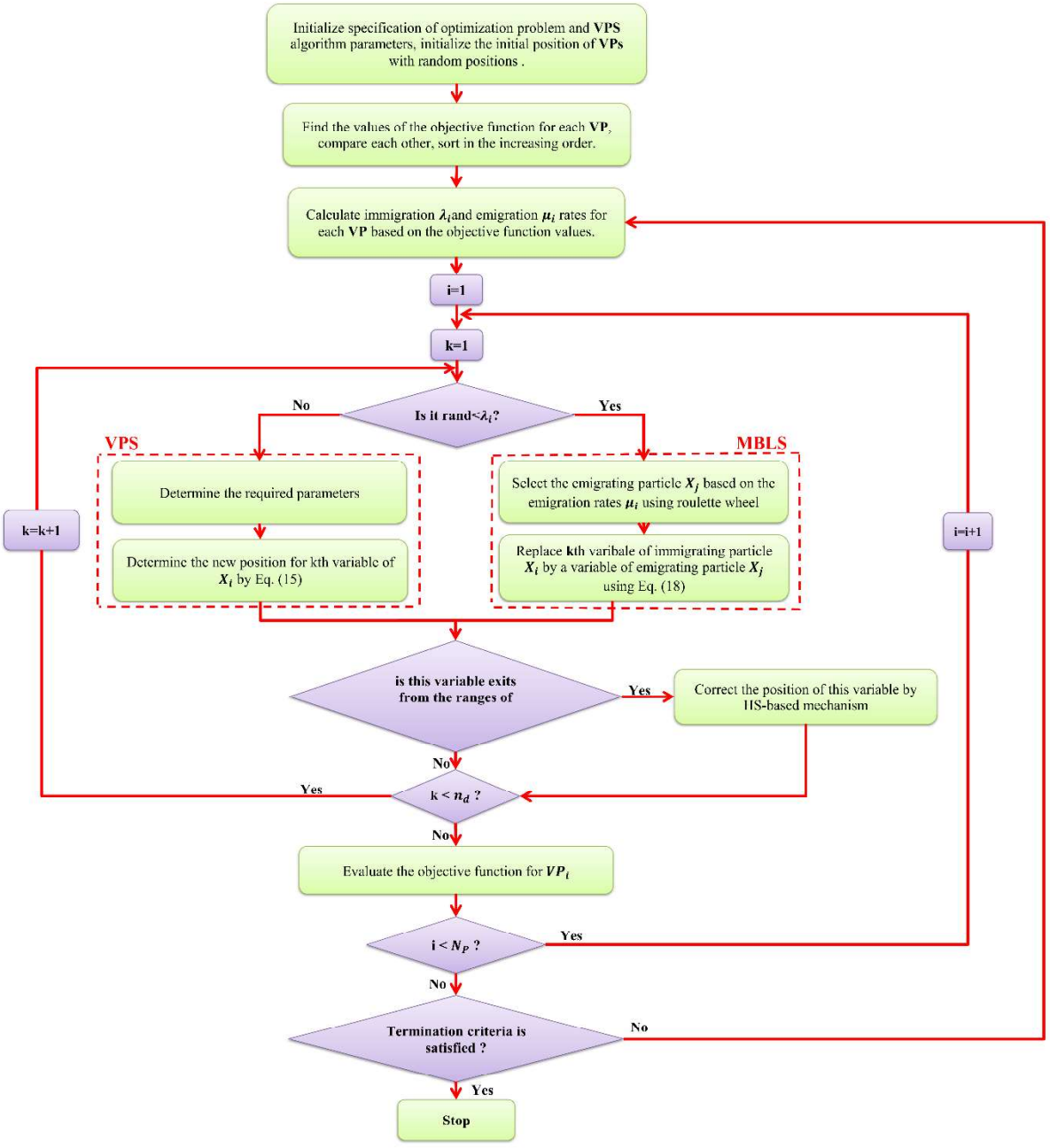

Fig. 4. The flowchart of the VPS-MBLS I (Parallel scheme).

4.2. VPS-MBLS with series scheme (VPS-MBLS II)

In the second hybrid approach, the VPS algorithm and MBLS mechanism are hybridized with series scheme as illustrated in Fig. 5. The main features of this hybridizing scheme are listed below.

- The new position for all of the VPs in the considered search space are determined by the standard VPS algorithm.
- The new position of the VPs are determined by the MBLS mechanism with the probability of λ_i, right after the movement of each VP in the search space toward the global optimum regions considering the standard VPS algorithm.
- The MBLS mechanism is utilized in order to exploit the generated VP by the VPS algorithm in a strong manner even if this selection process is conducted randomly based on the considered immigration rates (λ_i). In other words, this process is applied probabilistically as a local search mechanism which is considered as an embedded component to exploit promising areas considered by the VPS algorithm.

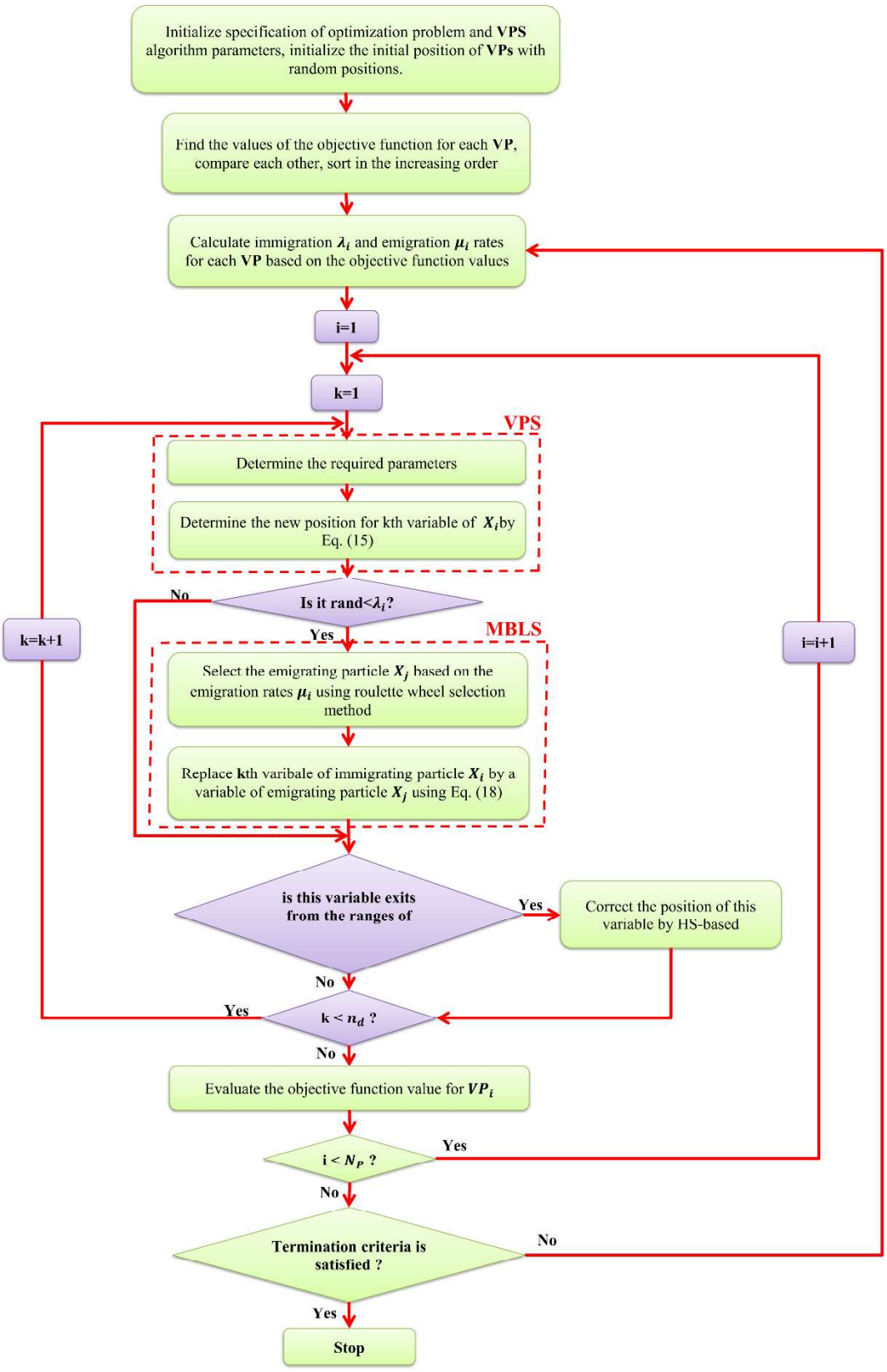

Fig. 5. The flowchart of the VPS-MBLS II (Series scheme).

4.3. VPS-MBLS with mixed parallel and series scheme (VPS-MBLS-III)

The last hybrid approach is a mixed hybridizing of the first and second hybrid algorithms. The flowchart of third algorithm is illustrated by Fig. 6. The proposed hybrid algorithms allow the VPs to profit not only from their own discoveries and the discoveries of the swarm as a whole, but also from the discoveries of the VPs with better fitness in each generation. With both VPS and MBLS techniques, proposed hybrid algorithms can balance exploration and exploitation, and efficiently deal with complicated problems.

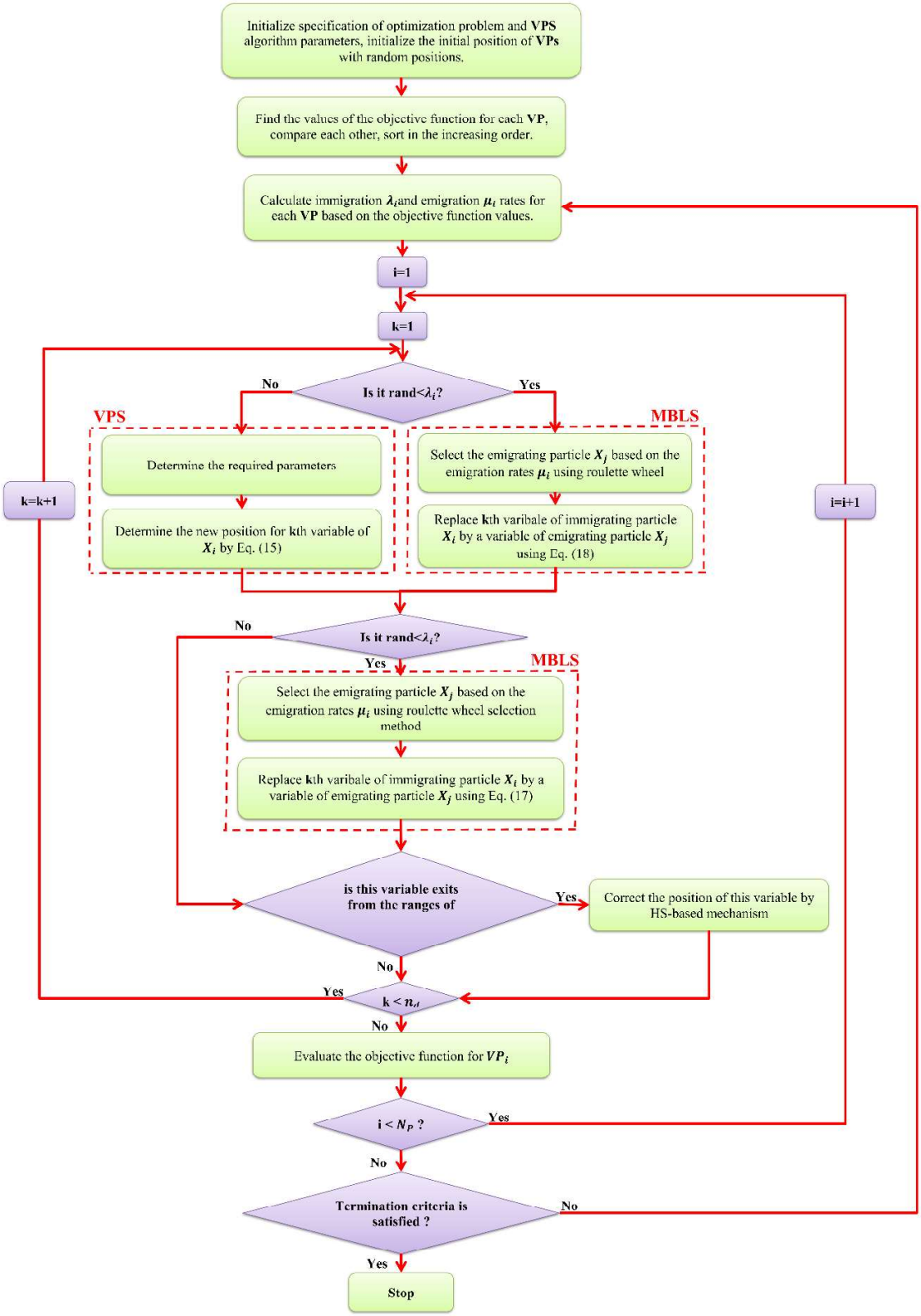

Fig. 6. The flowchart of the VPS-MBLS III (Mixed scheme).

5. Design Examples

In this section, the descriptive information for the one benchmark frame structure and two real-size steel building structures are provided which are utilized for determining the capability of the hybrid and standard metaheuristic algorithms in evaluating the optimum design sections of the structural elements. These structures are selected by different plans and in different heights in order to determine the effectiveness of the improved optimization algorithm in dealing with various kinds of building structures. In these structures, the material properties are taken as stainless steel with the modulus of elasticity (E) equal to 200 GPa, yield stress (F_y) equal to 248.2 Mpa, and unit weight of the steel (q) equal to 7.85 ton/m^3.

For design purposes, the considered building structures are subjected to 10 load combinations which are presented in Table 1. The acting dead and live loads on the typical floor beams are considered as 14 and 10 kN/m respectively while for the roof beams, the dead loads and live loads are determined as 12 and 7 kN/m respectively. The seismic and wind loads for the considered structural systems are all determined based on the ASCE 7-05 [41] which represents the minimum design loads for buildings and other structures.

For design purposes, the essential data for design proposes are all derived of the AISC-LRFD [28] steel design code. In addition, based on the fact that these examples are developed by Kazemzadeh Azad and Hasançebi [23,24] for the first time, the detailed information regarding the load, the allowable inter-story drift ratio, seismic force-resisting systems type, over strength factor, seismic design category and the other important criteria and parameters are as presented in [23,24]. Besides, the profile list for sizing purposes is selected from standard W-sections as suggested by Refs [23-25].

Table 1. Load combinations for steel structural design.

No.	***Combination***
1	$1.4\,D$
2	$1.2\,D + 1.6\,L$
3	$1.2\,D + 1.0\,E_x + 0.5\,L$
4	$1.2\,D + 1.0\,E_{ex} + 0.5\,L$
5	$1.2\,D + 1.0\,E_y) + 0.5\,L$
6	$1.2\,D + 1.0\,E_{ey} + 0.5\,L$
7	$0.9\,D + 1.0\,E_x$

8	$0.9\,D + 1.0\,E_{ex}$
9	$0.9\,D + 1.0\,E_{y}$
10	$0.9\,D + 1.0\,E_{ey}$

D: Dead Load, L: Live Load, E: Earthquake Load,
x and y: Loading Directions without eccentricity.
ex and ey: Loading Directions with eccentricity.

5.1. Benchmark 3-bay 24-story steel frame [42]

This example is a frame structure that consists of 100 joints and 168 members as presented in Fig. 7. The columns are considered as non-braced along their length, and the unbraced length for beam members are considered as one-fifth of the span length. To impose fabrication conditions, the beams of the first and third bay except the roof are categorized in one group, which results in four beam groups. The exterior columns are categorized into one group and the interior columns are considered together in another group that changes in every three stories. This grouping results in 16 column groups chosen from 267 W-shape sections and 4 beam groups selected from 37 of W14 sections.

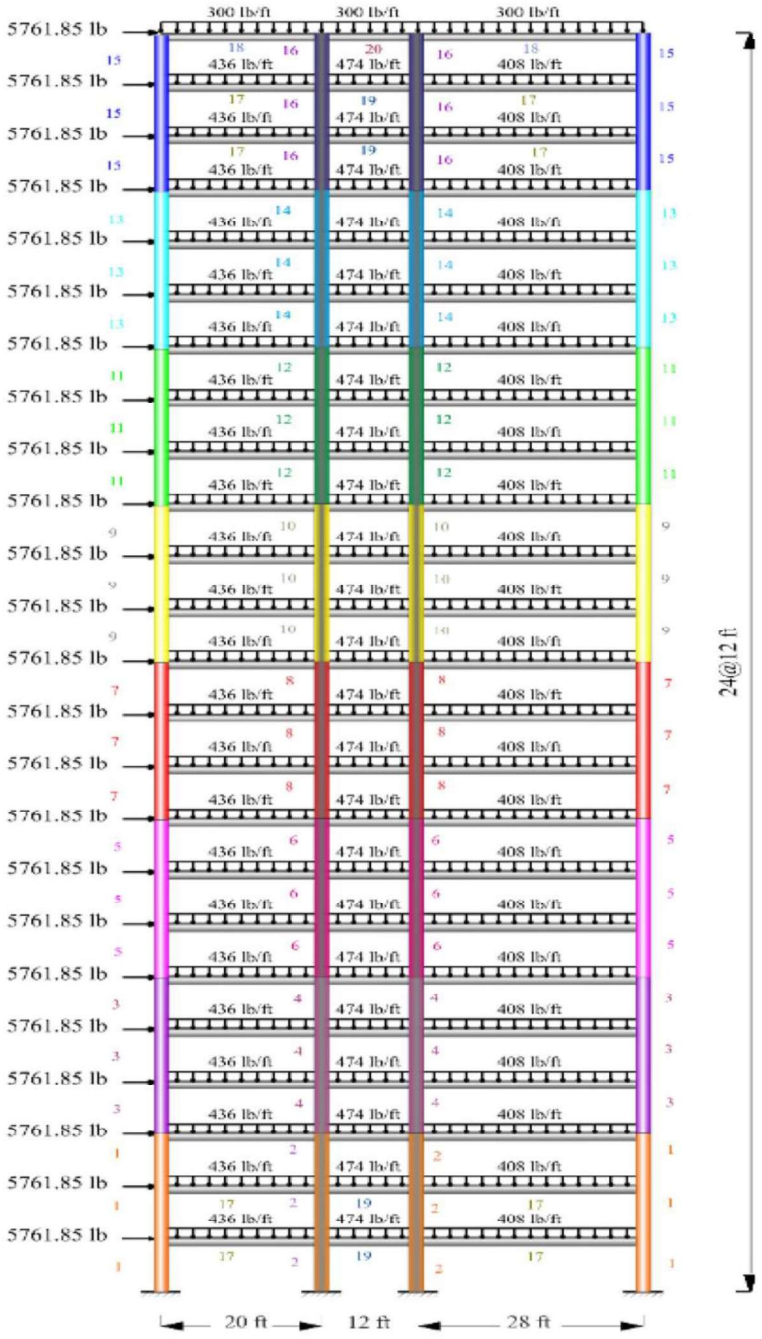

Fig. 7. The 3-bay 24-story frame structure

5.2. Example 2: 10-story, 1026-member steel structure [23]

A 10-story steel building structure is considered as the second design example which has 1026 structural members. This design example includes 350 columns, 580 beams, and 96 bracing elements in which the design sections for the columns, beams and braces are considered as

standard W-shaped sections. The lateral stability of this structure is provided through cross bracing systems along the *X* and *Y* directions alongside the moment resisting connections. The schematic view of this structure is illustrated in Fig. 8 while the plan and elevation views of this building are depicted in Figs. 9 and 10 according to the *X* and *Y* directions.

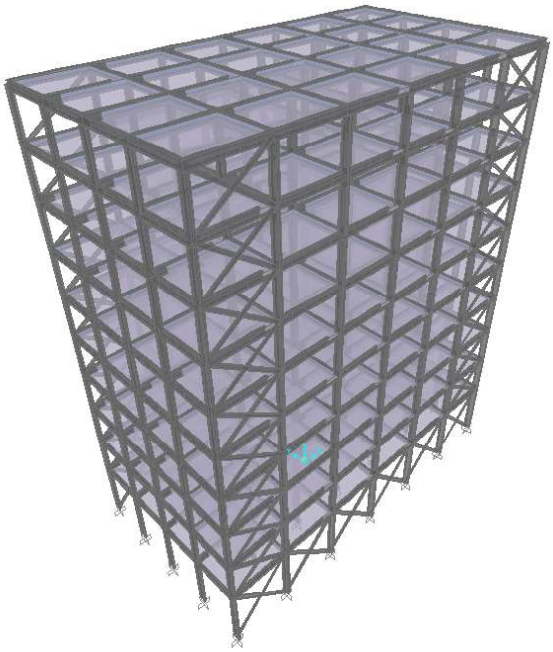

Fig. 8. The schematic view of the 10-story steel structure with 1026 members.

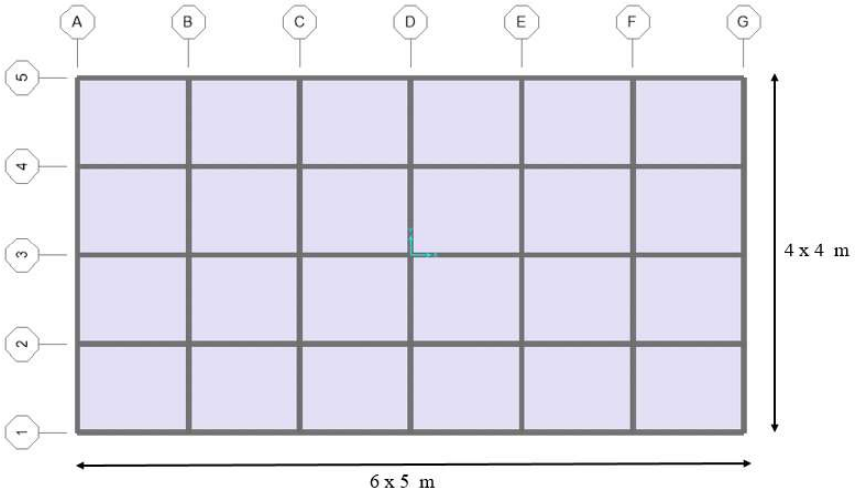

Fig. 9. The plan view of the 10-story steel structure with 1026 members.

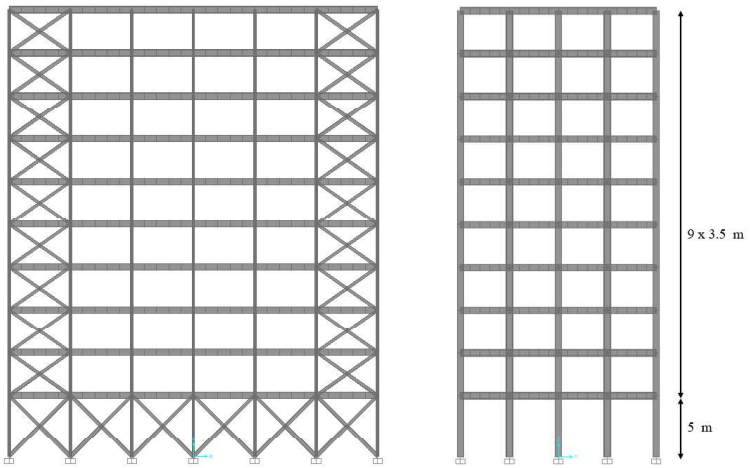

Fig. 10. The elevation views of the 10-story steel structure with 1026 members.

All of the 1026 structural members of the mentioned structure are determined in 32 member groups regarding the requirements for practical fabrication. Both plan and elevation levels are considered for member grouping while the structural elements are grouped regarding every three stories in elevation level except the first story which is determined separately. In addition, the columns are categorized into 5 different column groups in plan level as displayed in Fig. 11. For beam elements, two design groups are considered regarding the outer and inner beams while bracings are supposed to be in one design group. Therefore, there are a complete set of twenty column groups, eight beam groups, and four bracing groups which are considered based on both plan and elevation level groupings.

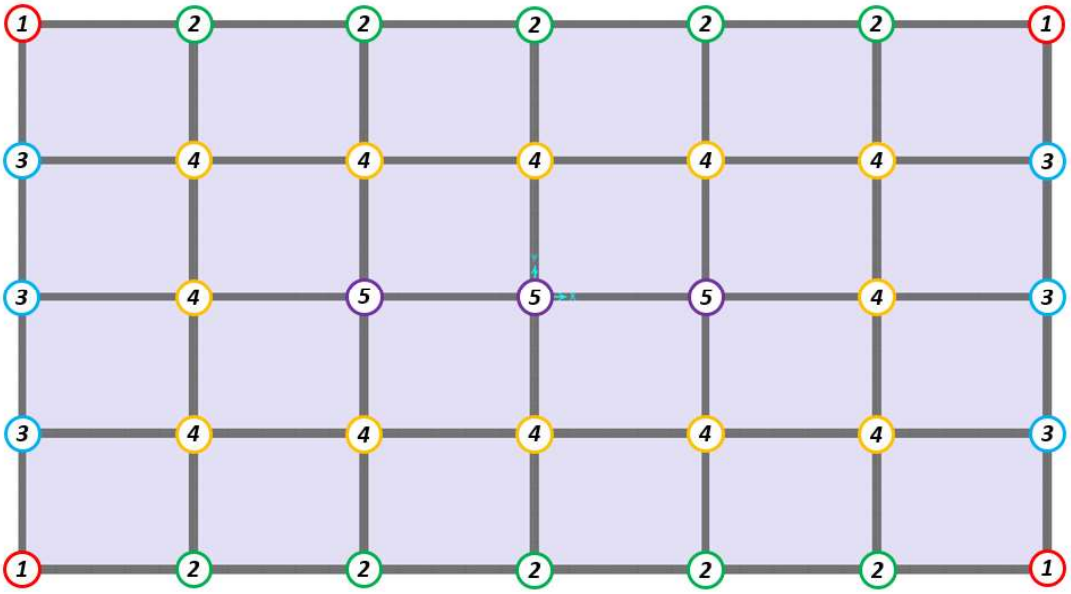

Fig. 11. Column grouping of the 10-story steel structure with 1026 members.

5.3. Example 3: 20-story, 3860-member steel structure [24]

The third design problem is determined as a 20-story steel building structure with 3860 structural members. This design example includes 1064 columns, 1836 beams, and a total number of 960 elements for bracings in which the design sections for the columns, beams and braces are considered as standard W-shaped sections. The lateral resistance of this structure is delivered through cross bracing systems in the *X* and *Y* directions alongside the moment resisting connections. The schematic and plan views of this structure are illustrated in Fig. 12. The elevation views of this building are depicted in Figs. 13 and 14 according to *X* and *Y* directions.

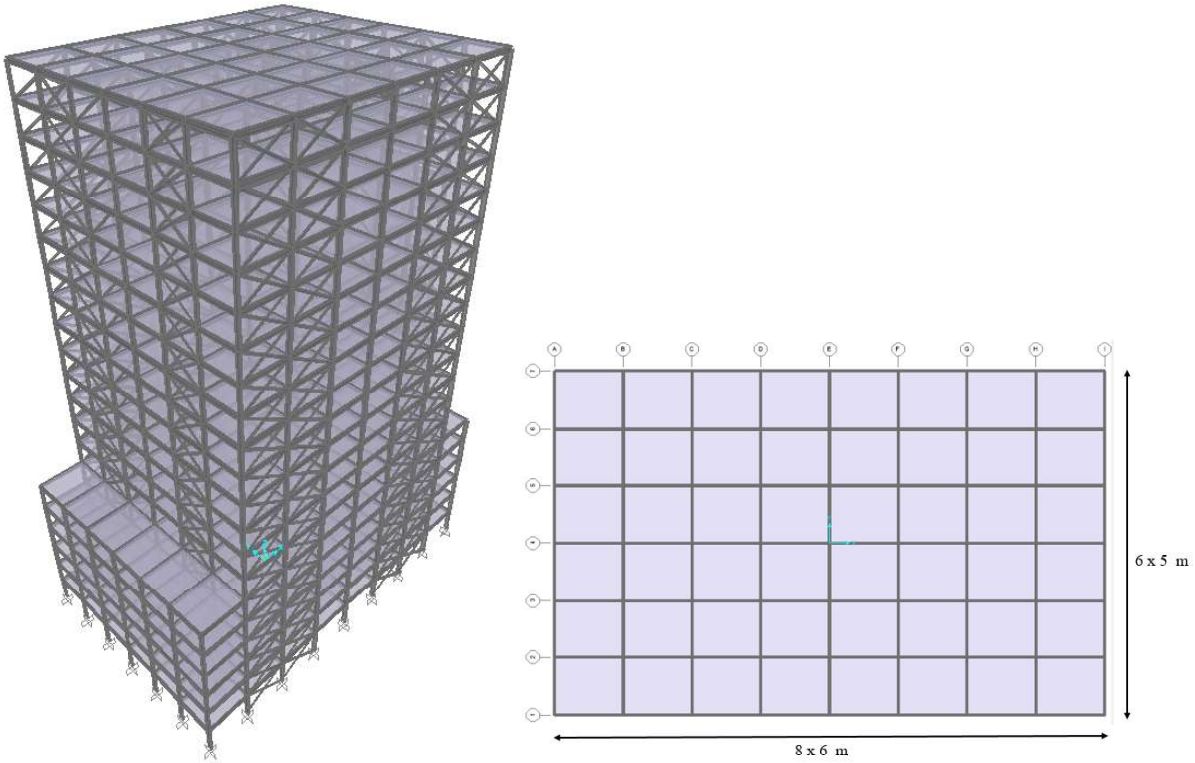

Fig. 12. The schematic and plan views of the 20-story steel structure with 3860 members.

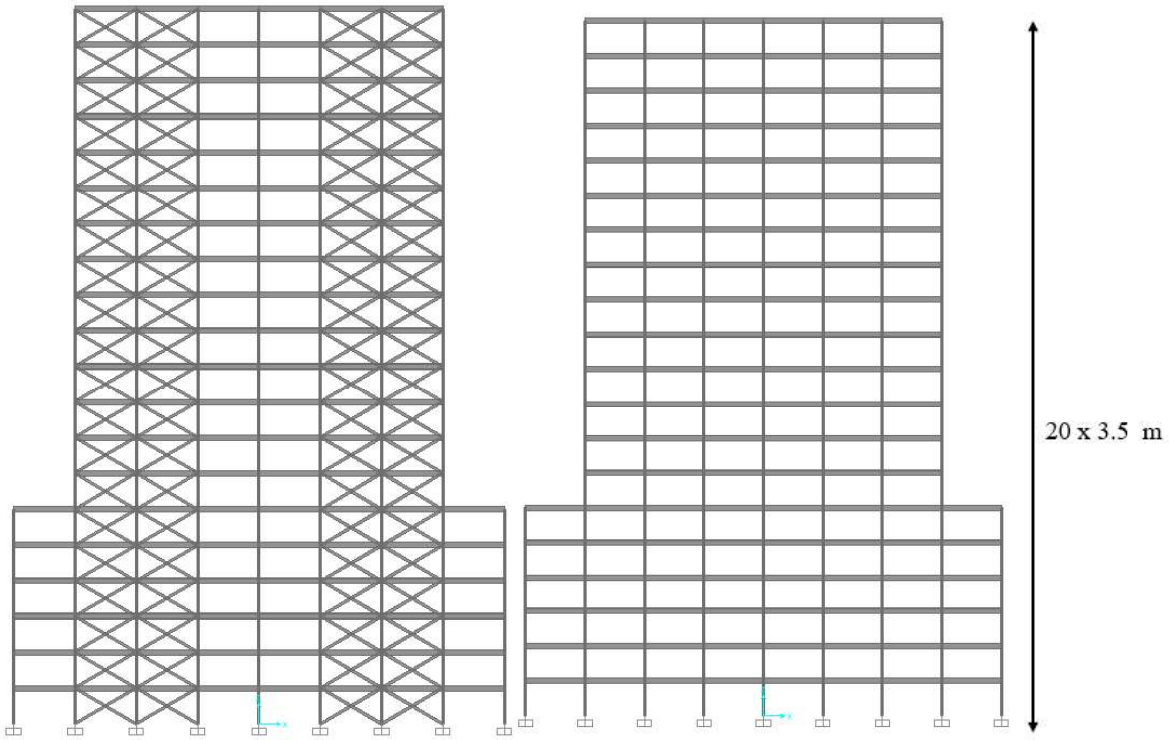

Fig. 13. The elevation views of the 20-story steel structure with 3860 members in *X* direction.

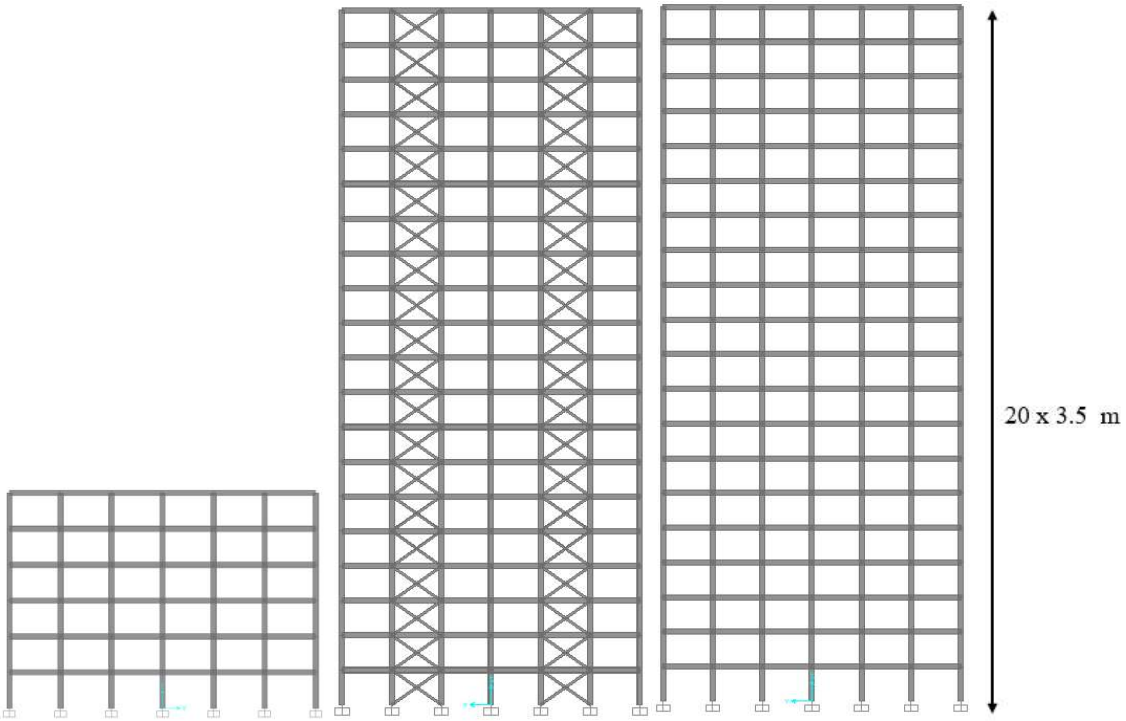

Fig. 14. The elevation views of the 20-story steel structure with 3860 members in *Y* direction.

All of the 3860 structural members of the 20-story steel structure are determined in 73 member groups regarding the requirements for practical fabrication. Both plan and elevation levels are considered for member grouping while the structural members in the elevation level are grouped in every two stories. Also, the columns are considered in 5 different groups in plan level as displayed in Fig. 15. For beams, two groups are considered for the inner and outer beams while for the bracings, one group is determined for each of the adjacent two stories of the structure. As a result, a total number of 43 column design groups, 20 beam design groups, and 10 bracing design groups are considered based on the plan and elevation levels of the structure.

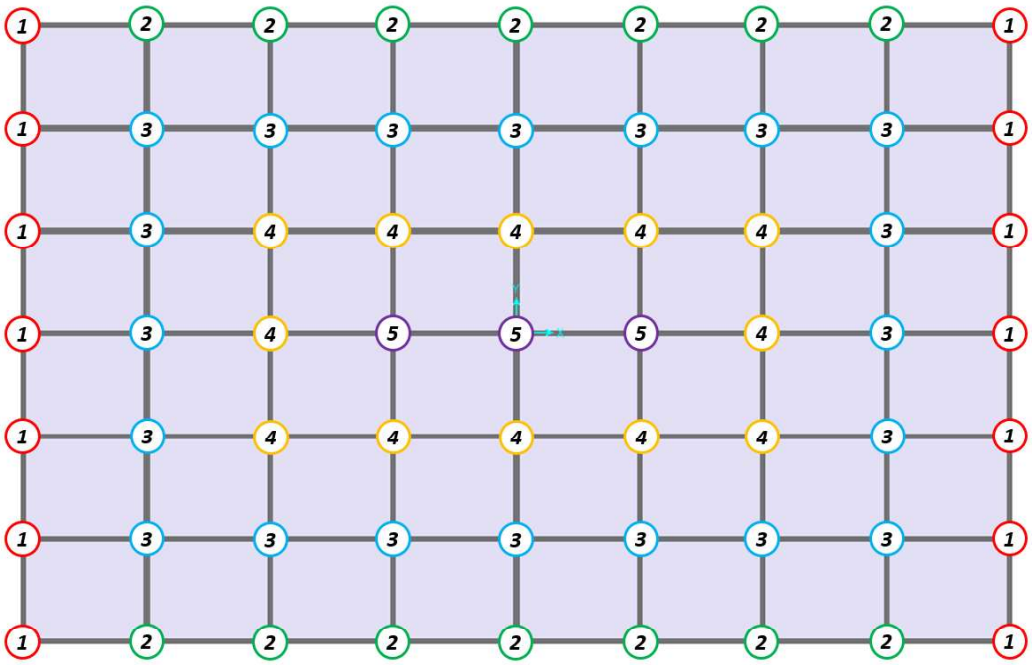

Fig. 15. Column grouping of the 20-story steel structure with 3860 members.

6. Numerical Results

In this section the numerical results of different approaches in dealing with the benchmark and real size building structure are provided.

6.1. Results of Benchmark Frame

For the benchmark frame structure of 24- story frame, the results of the weight optimization process for the proposed hybrid approaches are presented in Table 2 in which the results of other metaheuristics are also provided for comparative purposes. Based on the results, it can be concluded that the proposed hybrid methods are capable of providing better results than the other well-known metaheuristic algorithms.

Table 2. Optimum results for the 24-story benchmark structure.

	VPS	*BBO*	*Hybrid VPS-MBLS I*	*Hybrid VPS-MBLS II*	*Hybrid VPS-MBLS III*

Best Weight (kip)	**215.23**	**218.68**	**207.36**	**208.86**	**204.20**
Average Weight (Kip)	**245.97**	**250.77**	**226.85**	**222.99**	**214.36**
Std	**20.58**	**22.68**	**15.36**	**12.69**	**10.55**

6.2. Results of Real-Size Buildings

In this section, the numerical results for the weight optimization process of the selected 10- and 20-story steel structures are presented. The convergence history for the best results of hybrid VPS-MBLS approaches alongside the standard VPS and BBO algorithms for the 10- and 20-story structures are presented in Figs 16 and 17, respectively. It should be noted that the VPS-MBLS III is capable of converging to better results than the other hybrid and standard approaches with minimum number of required structural analysis. The required number of analyses for the standard algorithms are set to 21.000 and 25.000 for the 10- and 20-story frames, respectively. The convergence histories show that 11.000 and 20.000 are sufficient for the hybrid new methods.

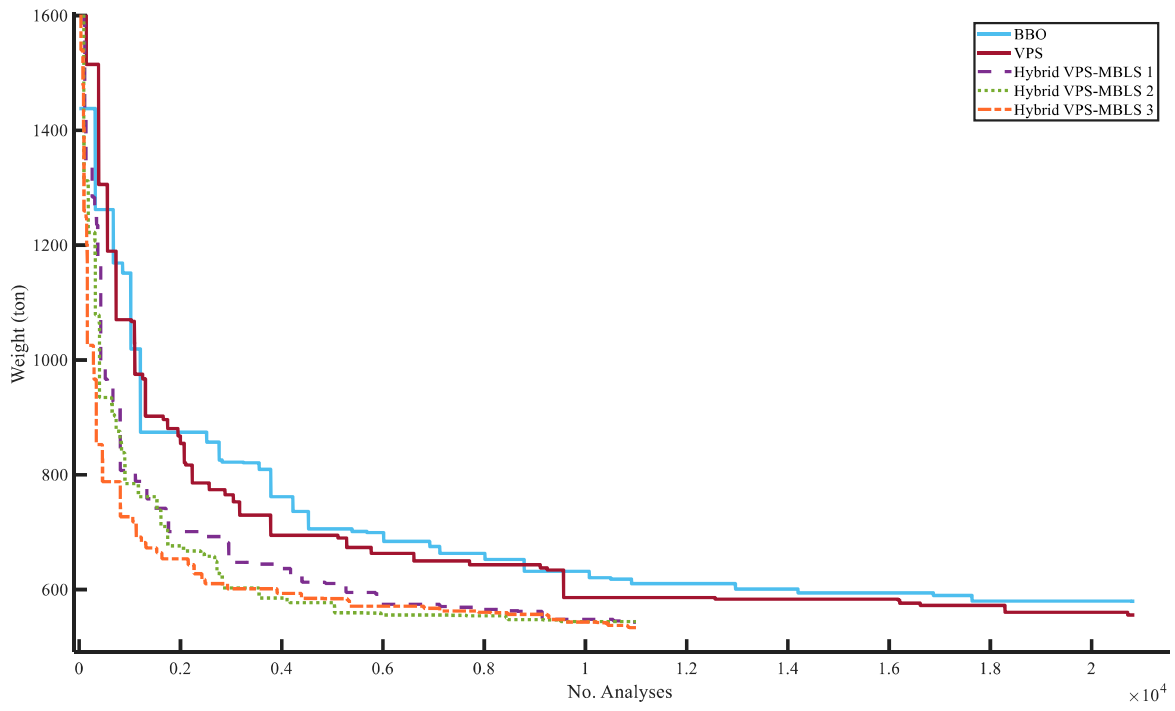

Fig. 16. Convergence history of the hybrid VPS-MBLS approaches and the standard algorithms for the 10-story structure.

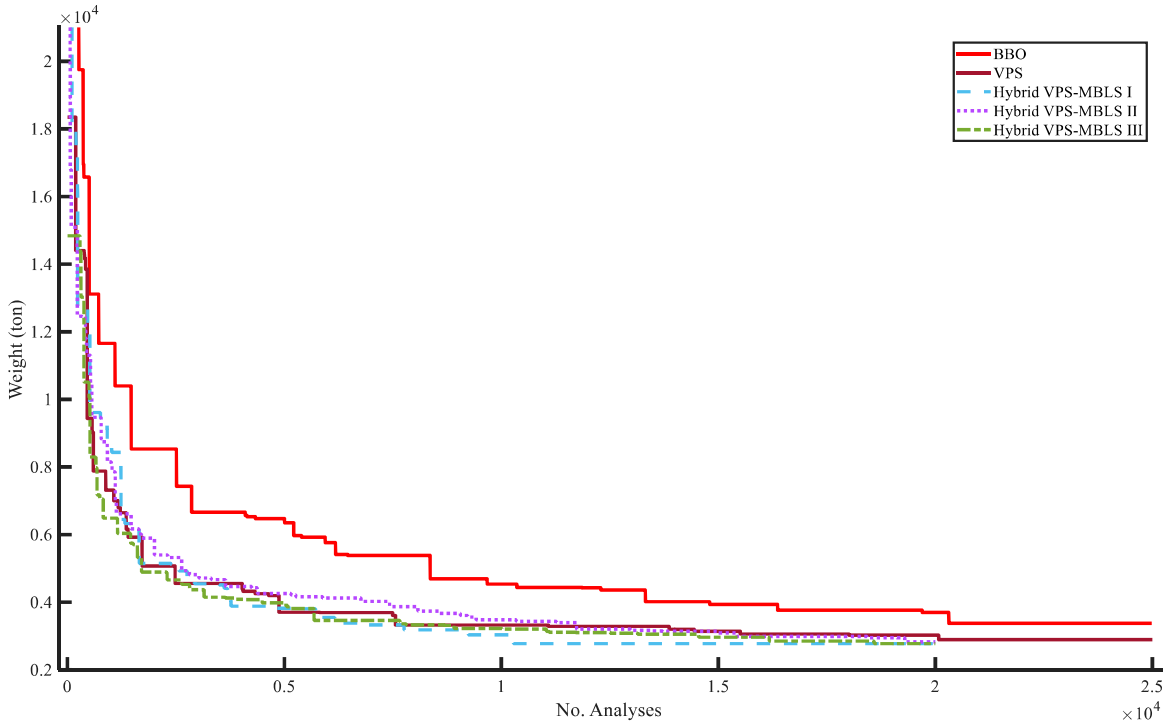

Fig. 17. Convergence history of the hybrid VPS-MBLS approaches and the standard algorithms for the 20-story structure.

The optimum design sections obtained by the hybrid VPS-MBLS approaches and the standard algorithms for the 10-story steel structures are presented in Table 3. The total weight for the 10-story steel structure considering the VPS-MBLS III approach is calculated as 534.112 ton which is the best value among other method that are 555.64, 579.85, 544.18, and 545.06 ton for the VPS-MBLS I, VPS-MBLS II, standard VPS and standard BBO approaches, respectively.

Based on the fact that this design example was considered by different authors using different metaheuristic approaches, the comparative results of the proposed methods and other algorithms are provided in Table 4. It should be noted that the VPS-MBLS III approach is capable of providing better results than the other standard and hybrid ones; however, it is 5.4 % heavier that the reported result by Kazemzadeh Azad [25] using Monitored Convergence Curve Integrated (MCC-MB) approach. It should be noted that the developed algorithm needs only 11.000 analyses to find the final optimum design that is 4.54% less that required number

of analyses for the MCC-MB [25] (i.e. 50.000 analyses). The average result of MCSS-MB in the 11.000th analyses is equal to 591.92 that is 9.52% more than the average result of the new method.

Table 3. Optimum design sections for the 10-story steel structure with 1026 members.

Stories	***Groups***	***VPS***	***BBO***	***Hybrid VPS-MBLS I***	***Hybrid VPS-MBLS II***	***Hybrid VPS-MBLS III***
1	*CG_1*	*W40X466*	*W40X593*	*W40X277*	*W24X229*	*W36X245*
	CG_2	*W40X215*	*W36X194*	*W36X150*	*W44X230*	*W24X117*
	CG_3	*W24X131*	*W16X100*	*W33X152*	*W12X106*	*W24X176*
	CG_4	*W27X146*	*W33X169*	*W36X182*	*W36X230*	*W40X174*
	CG_5	*W21X147*	*W24X207*	*W36X150*	*W24X229*	*W21X132*
	IB	*W8X21*	*W8X18*	*W8X18*	*W16X31*	*W8X18*
	OB	*W18X40*	*W16X26*	*W30X90*	*W21X44*	*W33X152*
	BR	*W14X82*	*W8X67*	*W18X76*	*W24X62*	*W8X31*
2-4	*CG_1*	*W33X263*	*W30X261*	*W33X241*	*W36X256*	*W36X245*
	CG_2	*W40X167*	*W21X122*	*W18X119*	*W36X150*	*W36X160*
	CG_3	*W14X99*	*W40X174*	*W21X111*	*W33X152*	*W30X124*
	CG_4	*W33X130*	*W21X101*	*W36X170*	*W30X132*	*W21X111*
	CG_5	*W14X120*	*W24X117*	*W16X100*	*W27X129*	*W18X130*
	IB	*W27X94*	*W24X55*	*W27X84*	*W24X68*	*W24X68*
	OB	*W18X46*	*W30X108*	*W16X45*	*W14X30*	*W24X62*
	BR	*W8X58*	*W24X68*	*W14X68*	*W24X68*	*W10X77*
5-7	*CG_1*	*W21X166*	*W12X106*	*W27X114*	*W33X169*	*W40X167*
	CG_2	*W14X120*	*W24X117*	*W14X159*	*W21X111*	*W14X145*
	CG_3	*W36X160*	*W18X86*	*W27X129*	*W30X90*	*W30X116*
	CG_4	*W14X193*	*W30X211*	*W18X76*	*W14X159*	*W16X77*
	CG_5	*W18X71*	*W18X175*	*W12X79*	*W30X148*	*W16X100*
	IB	*W24X62*	*W18X76*	*W18X50*	*W24X62*	*W18X40*
	OB	*W21X68*	*W18X40*	*W30X132*	*W30X108*	*W33X130*
	BR	*W8X40*	*W14X53*	*W12X53*	*W12X53*	*W18X60*
8-10	*CG_1*	*W18X40*	*W18X97*	*W16X31*	*W12X50*	*W27X102*
	CG_2	*W12X58*	*W21X73*	*W14X145*	*W12X65*	*W14X109*
	CG_3	*W16X57*	*W14X90*	*W21X68*	*W12X79*	*W24X94*
	CG_4	*W21X122*	*W14X193*	*W24X104*	*W24X162*	*W33X141*
	CG_5	*W16X77*	*W40X167*	*W14X61*	*W12X190*	*W16X45*
	IB	*W18X55*	*W16X50*	*W18X46*	*W21X57*	*W21X50*
	OB	*W16X36*	*W27X94*	*W16X40*	*W8X18*	*W12X30*
	BR	*W14X90*	*W14X38*	*W24X62*	*W12X50*	*W12X65*
Weight		***555.64***	***579.85***	***544.18***	***545.06***	***534.11***
Maximum Drift Ratio		***0.9944***	***0.9901***	***0.9649***	***0.9984***	***0.9764***
Max Displacement of Top Story (mm)		***73.6***	***71.8***	***73.6***	***73.1***	***73.5***
Max Stress Ratio		***0.9281***	***0.9319***	***0.8847***	***0.8250***	***0.9926***

CG_{1-5}: *Column Groups 1 to 5 (Fig. 10).*
IB: *Inner Beam Group.*
OB: *Outer Beam Group.*

BR: *Bracing Group.*

Table 4. Comparative results for the 10-story steel structure with 1026 members.

Metaheuristics	*Total Weight (ton)*	*Required Number of Analyses*
UEBB-BC [23]	*584.93*	*25000*
ACSS [45]	*540.38*	*21.000*
ALO-JA [43]	*548.36*	*25000*
ICHHO [44]	*552.36*	*25000*
HS/BBBC/SA [36]	*561.98*	*25000*
MCC-MB [25]	*504.34*	*50.000*
VPS	*555.64*	*25.000*
BBO	*579.85*	*25.000*
Hybrid VPS-MBLS I	*544.18*	*11.000*
Hybrid VPS-MBLS II	*545.06*	*11.000*
Hybrid VPS-MBLS III	*534.11*	*11.000*

UEBB-BC: *Upper bound Exponential Big Bang-Big Crunch*

CSS: *Charged System Search*

ACSS: *Advanced Charged System Search*

MCC-MB*: Monitored Convergence Curve Integrated II*

In Fig. 18, the analysis of variance is conducted for the statistical results of different approaches in dealing with the 10-story steel building structure by considering 30 independent optimization runs. It is obvious that the third hybrid approaches is capable of providing lower results than the other approaches.

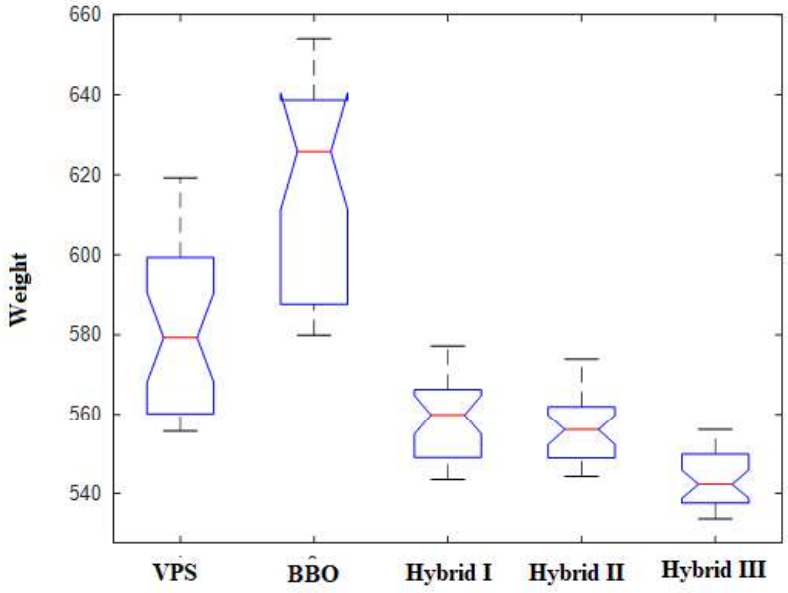

Fig. 18. The results of analysis of variance for 10-story building.

The optimum design sections obtained by the hybrid VPS-MBLS approaches and the standard algorithms for the 20-story steel structures are presented in Table 5. The total weight for the 20-story steel structure considering the VPS-MBLS III approach is calculated as 2787.50 ton which is the best value between other methods. For the VPS-MBLS I, VPS-MBLS II, standard VPS and standard BBO approaches, this value is calculated as 2812.94, 2799.49, 2917.42 and 3276.96 ton, respectively.

The comparative results of the new methods and the other algorithms proposed by other researchers [24, 25] are provided in Table 6. Clearly, the VPS-MBLS III approach is capable of providing the best results compared to the other approaches. The required number of analyses is 50.000 for the MCC-EB [25] while it is 20.000 for the new method and the result of VPS-MBLS III is 185.14 ton less than MCC-EB algorithm.

Table 5. Optimum design sections for the 20-story steel structure with 3860 members.

Stories	Groups	VPS	BBO	Hybrid VPS-MBLS I	Hybrid VPS-MBLS II	Hybrid VPS-MBLS III
1-2	CG_1	W14X48	W27X217	W18X97	W8X48	W24X131
	CG_2	W36X230	W36X280	W33X141	W30X173	W14X145
	CG_3	W40X321	W33X241	W14X233	W12X170	W24X335
	CG_4	W14X455	W14X730	W27X307	W40X235	W14X500
	CG_5	W24X117	W36X160	W18X158	W30X132	W21X132
	IB	W14X61	W14X99	W21X73	W24X68	W12X79
	OB	W12X72	W16X57	W33X141	W24X117	W24X84
	BR	W27X102	W24X94	W12X96	W8X48	W12X65
3-4	CG_1	W16X89	W18X71	W21X166	W18X76	W12X53
	CG_2	W18X234	W10X112	W33X130	W36X439	W33X169
	CG_3	W33X201	W33X318	W14X455	W30X292	W24X492
	CG_4	W27X307	W27X258	W24X335	W40X249	W36X260
	CG_5	W24X131	W36X135	W12X152	W24X117	W14X132
	IB	W12X65	W24X68	W14X48	W24X84	W14X48
	OB	W30X99	W30X292	W30X90	W21X62	W14X48
	BR	W12X72	W10X45	W18X71	W12X45	W10X88
5-6	CG_1	W14X74	W36X245	W12X136	W14X132	W14X48
	CG_2	W33X221	W21X101	W21X122	W40X235	W10X112
	CG_3	W40X278	W36X170	W40X235	W30X173	W40X235
	CG_4	W40X211	W40X215	W18X234	W14X283	W30X326
	CG_5	W21X101	W27X84	W18X130	W12X252	W14X90
	IB	W27X94	W12X96	W14X68	W14X90	W18X71
	OB	W14X53	W27X178	W12X53	W16X57	W14X68
	BR	W24X76	W14X74	W10X49	W12X45	W10X112
7-8	CG_1	N.A.	N.A.	N.A.	N.A.	N.A.
	CG_2	W27X94	W27X114	W18X76	W30X211	W12X96
	CG_3	W24X162	W30X211	W44X290	W36X232	W40X278
	CG_4	W44X262	W27X161	W12X305	W24X250	W14X159
	CG_5	W10X77	W21X73	W40X278	W12X72	W21X132
	IB	W12X72	W33X118	W18X76	W30X116	W18X76
	OB	W18X65	W40X211	W12X50	W18X60	W24X250
	BR	W8X48	W14X82	W14X109	W16X67	W14X68
9-10	CG_1	N.A.	N.A.	N.A.	N.A.	N.A.
	CG_2	W12X79	W10X88	W16X77	W12X252	W33X169
	CG_3	W40X199	W40X249	W14X132	W27X235	W24X279
	CG_4	W40X593	W40X593	W30X261	W14X455	W24X408
	CG_5	W18X71	W14X68	W40X167	W18X97	W27X194
	IB	W30X99	W10X49	W14X90	W16X67	W33X118
	OB	W16X67	W14X53	W40X215	W30X99	W12X72
	BR	W16X100	W12X45	W16X67	W10X49	W8X40
11-12	CG_1	N.A.	N.A.	N.A.	N.A.	N.A.
	CG_2	W16X77	W18X192	W10X112	W21X101	W27X84
	CG_3	W40X331	W40X183	W30X211	W18X211	W36X160
	CG_4	W40X264	W14X550	W24X117	W12X96	W18X130
	CG_5	W8X48	W18X71	W21X132	W10X77	W16X89
	IB	W21X68	W30X116	W21X83	W44X230	W33X141
	OB	W24X94	W8X67	W18X86	W8X58	W18X97
	BR	W10X39	W8X40	W8X40	W12X72	W14X74
13-14	CG_1	N.A.	N.A.	N.A.	N.A.	N.A.

	CG_2	*W12X96*	*W14X120*	*W24X94*	*W14X132*	*W14X61*
	CG_3	*W40X167*	*W24X146*	*W10X100*	*W12X170*	*W12X72*
	CG_4	*W33X291*	*W40X235*	*W40X277*	*W18X97*	*W44X262*
	CG_5	*W24X94*	*W24X117*	*W14X90*	*W12X305*	*W16X89*
	IB	*W30X99*	*W40X199*	*W10X54*	*W18X55*	*W21X68*
	OB	*W12X190*	*W14X68*	*W24X146*	*W8X58*	*W10X54*
	BR	*W8X31*	*W12X40*	*W12X65*	*W10X39*	*W8X40*
15-16	CG_1	*N.A.*	*N.A.*	*N.A.*	*N.A.*	*N.A.*
	CG_2	*W40X149*	*W24X62*	*W27X129*	*W30X211*	*W36X170*
	CG_3	*W16X100*	*W18X211*	*W30X116*	*W33X130*	*W12X136*
	CG_4	*W18X143*	*W24X68*	*W12X190*	*W14X132*	*W40X183*
	CG_5	*W12X152*	*W27X94*	*W36X245*	*W36X245*	*W24X103*
	IB	*W18X86*	*W30X99*	*W30X108*	*W24X117*	*W18X60*
	OB	*W10X49*	*W40X277*	*W18X86*	*W10X88*	*W12X79*
	BR	*W10X39*	*W12X45*	*W8X31*	*W8X31*	*W8X31*
17-18	CG_1	*N.A.*	*N.A.*	*N.A.*	*N.A.*	*N.A.*
	CG_2	*W8X31*	*W14X38*	*W12X45*	*W30X116*	*W10X49*
	CG_3	*W21X83*	*W18X119*	*W27X129*	*W30X173*	*W27X194*
	CG_4	*W24X279*	*W14X99*	*W21X182*	*W16X57*	*W36X150*
	CG_5	*W30X326*	*W10X112*	*W24X279*	*W24X131*	*W27X146*
	IB	*W21X111*	*W10X88*	*W27X84*	*W18X86*	*W16X67*
	OB	*W30X124*	*W21X132*	*W24X84*	*W14X53*	*W18X86*
	BR	*W8X31*	*W8X35*	*W21X73*	*W8X31*	*W8X31*
19-20	CG_1	*N.A.*	*N.A.*	*N.A.*	*N.A.*	*N.A.*
	CG_2	*W24X131*	*W12X79*	*W18X258*	*W8X28*	*W16X57*
	CG_3	*W30X116*	*W18X65*	*W18X71*	*W33X130*	*W27X114*
	CG_4	*W12X35*	*W36X393*	*W27X94*	*W24X104*	*W12X120*
	CG_5	*W24X84*	*W14X176*	*W14X109*	*W12X79*	*W18X119*
	IB	*W30X116*	*W16X77*	*W24X68*	*W18X60*	*W12X53*
	OB	*W12X87*	*W27X94*	*W21X93*	*W10X112*	*W21X93*
	BR	*W24X76*	*W6X20*	*W6X20*	*W18X28*	*W8X24*
Weight		***2917.42***	***3276.96***	***2812.94***	***2799.49***	***2787.50***
Maximum Drift Ratio		***0.8274***	***0.7315***	***0.8694***	***0.8589***	***0.8734***
Max Displacement of Top Story (mm)		***116.41***	***94.08***	***131.39***	***127.89***	***125.70***
Max Stress Ratio		***0.9787***	***0.9863***	***0.9738***	***0.9984***	***0.100***

CG_{1-5}: *Column Groups 1 to 5 (Fig. 14).*
IB: *Inner Beam Group.*
OB: *Outer Beam Group.*
BR: *Bracing Group.*

Table 6. Comparative results for the 20-story steel structure with 3860 members.

Metaheuristics	***Total Weight (ton)***	***Required Number of Analyses***
UBS [24]	*4117.43*	*9979*
MCC-EB [25]	*2972.64*	*50.000*
ALO-JA [43]	*2910.62*	*25.000*

ICHHO [44]	*2852.36*	*25.000*
HS/BBBC/SA [36]	*2888.23*	*25.000*
VPS	*2917.42*	*25.000*
BBO	*3276.96*	*25.000*
Hybrid VPS-MBLS I	*2812.94*	*20.000*
Hybrid VPS-MBLS II	*2799.49*	*20.000*
Hybrid VPS-MBLS III	*2787.50*	*20.000*

UBS: *Upper Bound Strategy*

MCC-EB*: Monitored Convergence Curve Integrated I*

The statistical results of the optimum design procedure for different methods based on 30 independent runs are presented in Table 7 and Table 8. It is concluded that the proposed hybrid methods are capable of providing better results than the standard methods by considering the mean and standard deviation results. In addition, the results of the analysis of variance for the statistical data of the 30 independent runs considering 20-story structure are presented in Fig. 19 in which the superiority of the proposed hybrid approaches are presented.

Table 7. Statistical results for different methods based on 30 independent runs regarding 10 story building.

Stories	***Best***	***Mean***	***Worst***	***Std.***
UBS [23]	*517.71*	*551.71*	*581.01*	*15.45*
ALO-JA [43]	*548.36*	*567.32*	*579.36*	*17.52*
ICHHO [44]	*552.36*	*572.21*	*582.31*	*20.88*
HS/BBBC/SA [36]	*561.98*	*586.99*	*598.01*	*25.01*
MCC-EB [25]	*510.71*	*523.31*	*537.49*	*7.16*
VPS	*555.64*	*581.40*	*619.27*	*20.41*
BBO	*579.85*	*617.96*	*654.03*	*24.99*
Hybrid VPS-MBLS I	*544.18*	*557.88*	*577.17*	*9.34*
Hybrid VPS-MBLS II	*545.06*	*556.44*	*573.92*	*8.33*
Hybrid VPS-MBLS III	*534.11*	*543.65*	*556.05*	*6.57*

Table 8. Statistical results for different methods based on 30 independent runs regarding 20 story building.

Stories	*Best*	*Mean*	*Worst*	*Std.*
MCC-EB [25]	*2972.64*	*3245.55*	*3494.69*	*138.45*
ALO-JA [43]	*2910.62*	*3256.34*	*3401.2*	*158.20*
ICHHO [44]	*2852.36*	*3265.32*	*3425.25*	*170.69*
HS/BBBC/SA [36]	*2888.23*	*3301.32*	*3389.36*	*156.23*
VPS	*2917.42*	*3193.66*	*3535.83*	*206.96*
BBO	*3276.96*	*3584.89*	*3878.14*	*203.00*
Hybrid VPS-MBLS I	*2812.94*	*2993.11*	*3181.78*	*101.26*
Hybrid VPS-MBLS II	*2799.49*	*2983.98*	*3130.45*	*103.69*
Hybrid VPS-MBLS II	*2787.5*	*2927.05*	*3066.63*	*97.22*

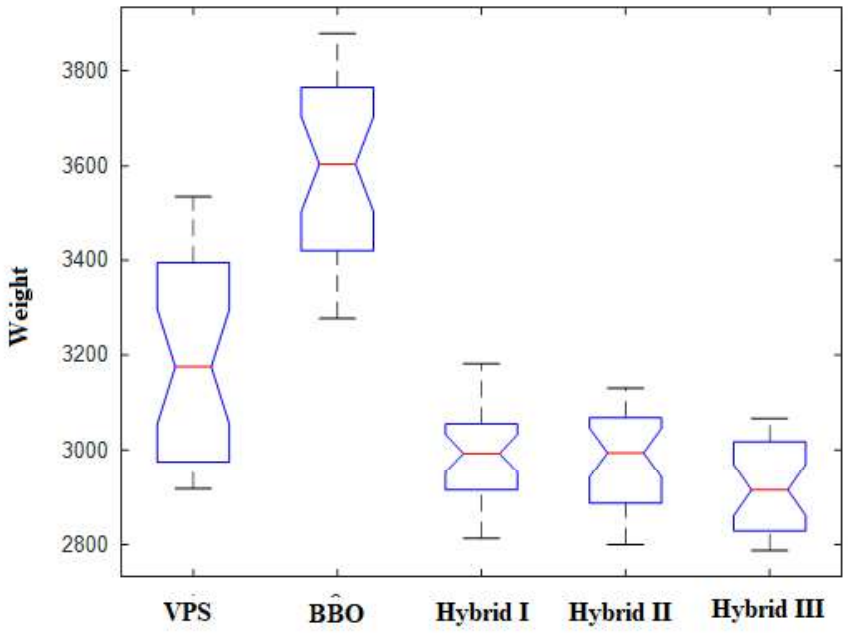

Fig. 19. The results of analysis of variance for 20-story building.

The maximum stress ratio of the groups of the structural elements for the 10-and 20-story design examples obtained by the proposed methods are depicted in Figs. 20 and 21, respectively. By considering the stress ratios in structural elements, it is concluded that the third hybrid approach (VPS-MBLS III) has higher stress values which represents that the

design procedure related to this method has the lowest possible design cross-sections concerning an economic design procedure.

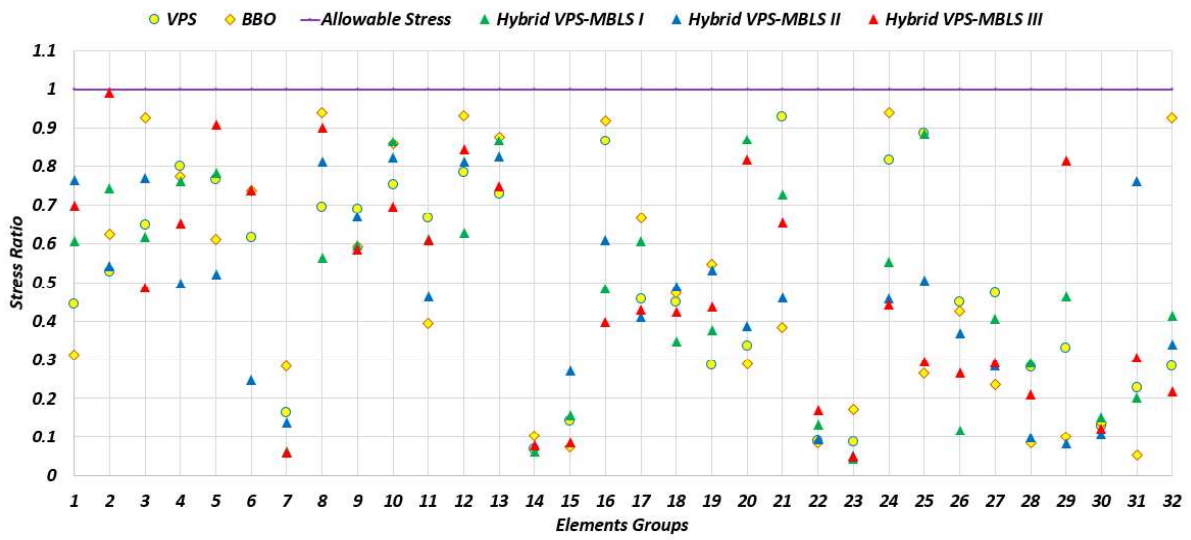

Fig. 20. The maximum stress ratio of the groups of elements for the 10-story design example.

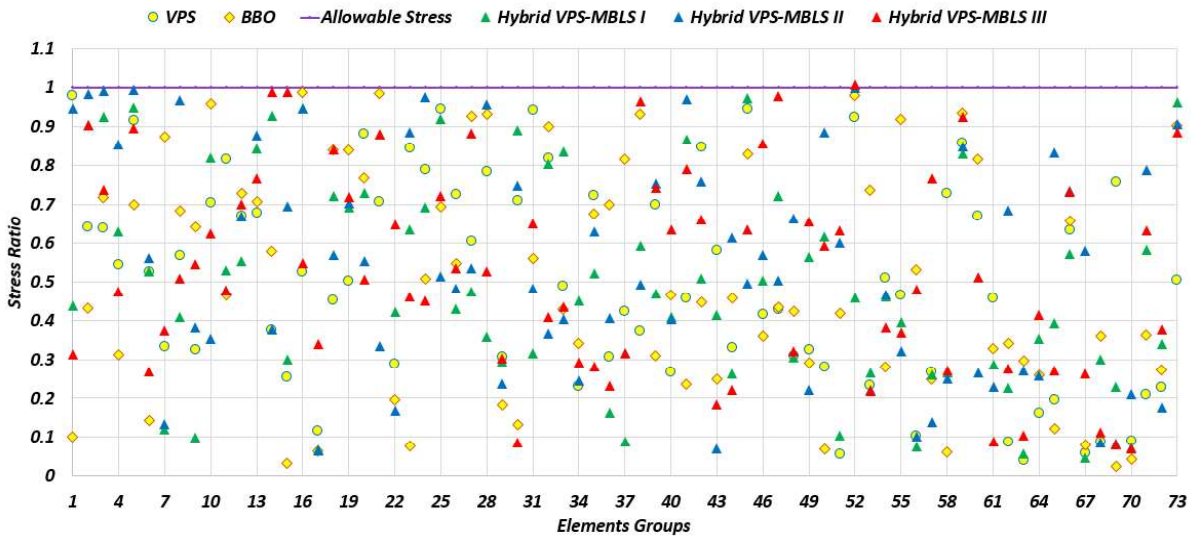

Fig. 21. The maximum stress ratio of the groups of elements for the 20-story design example.

The drift ratio of the optimum design obtained the proposed methods for 10- and 20-story building structures are depicted in Figs. 22 and 23, respectively f. It should be noted that for

the optimized structural design obtained by the hybrid approaches, drift ratios have higher values and near the allowable value which proves that the provided optimum design sections of the hybrid approaches (specially the VPS-MBLS III approach) have the lowest possible design cross-sections concerning an economic design procedure. It should be noted that the maximum drift ratio of the 10- and 20-story buildings are provided in Tables 2 and 3, respectively.

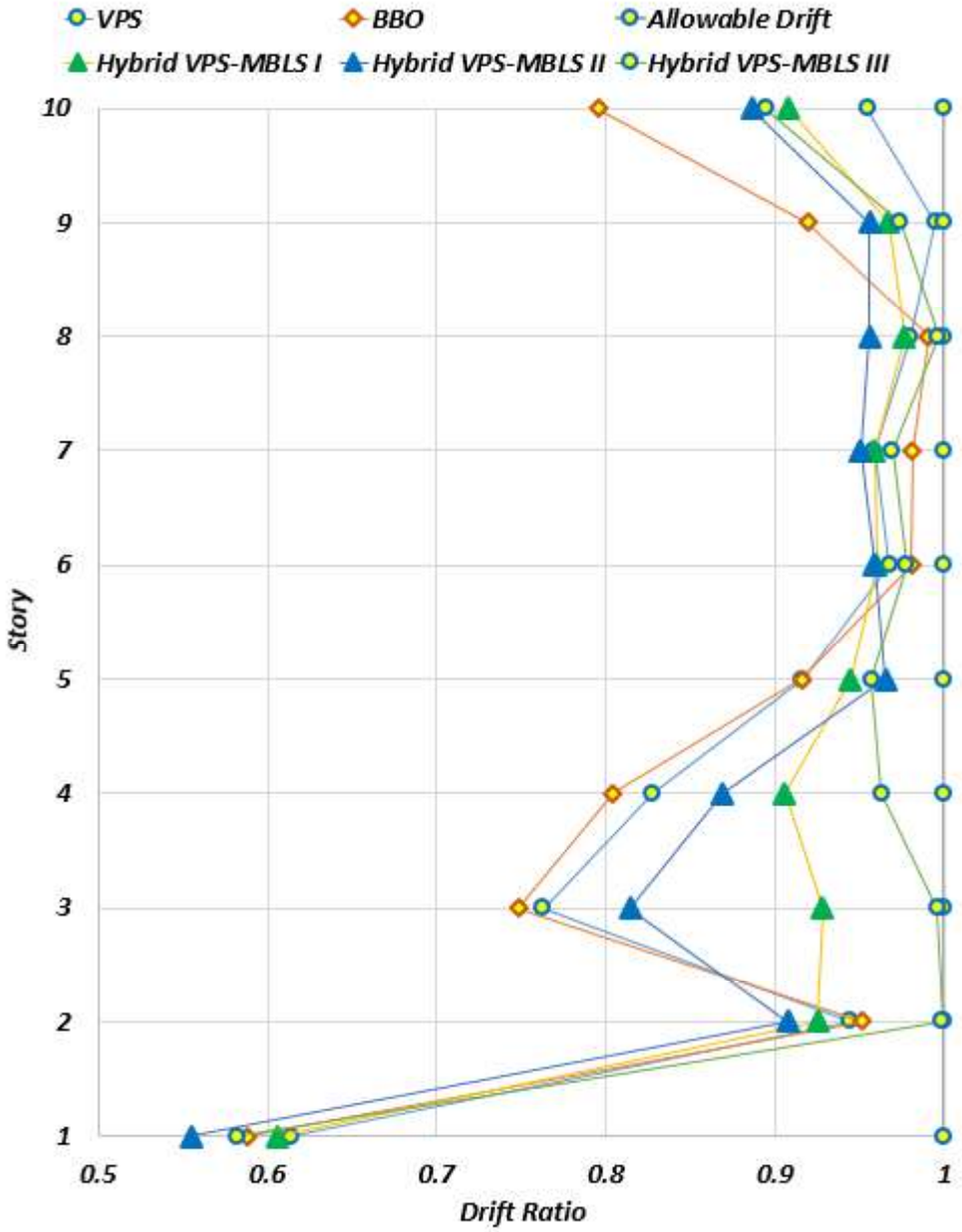

Fig. 22. The drift ratio of the 10-story design example.

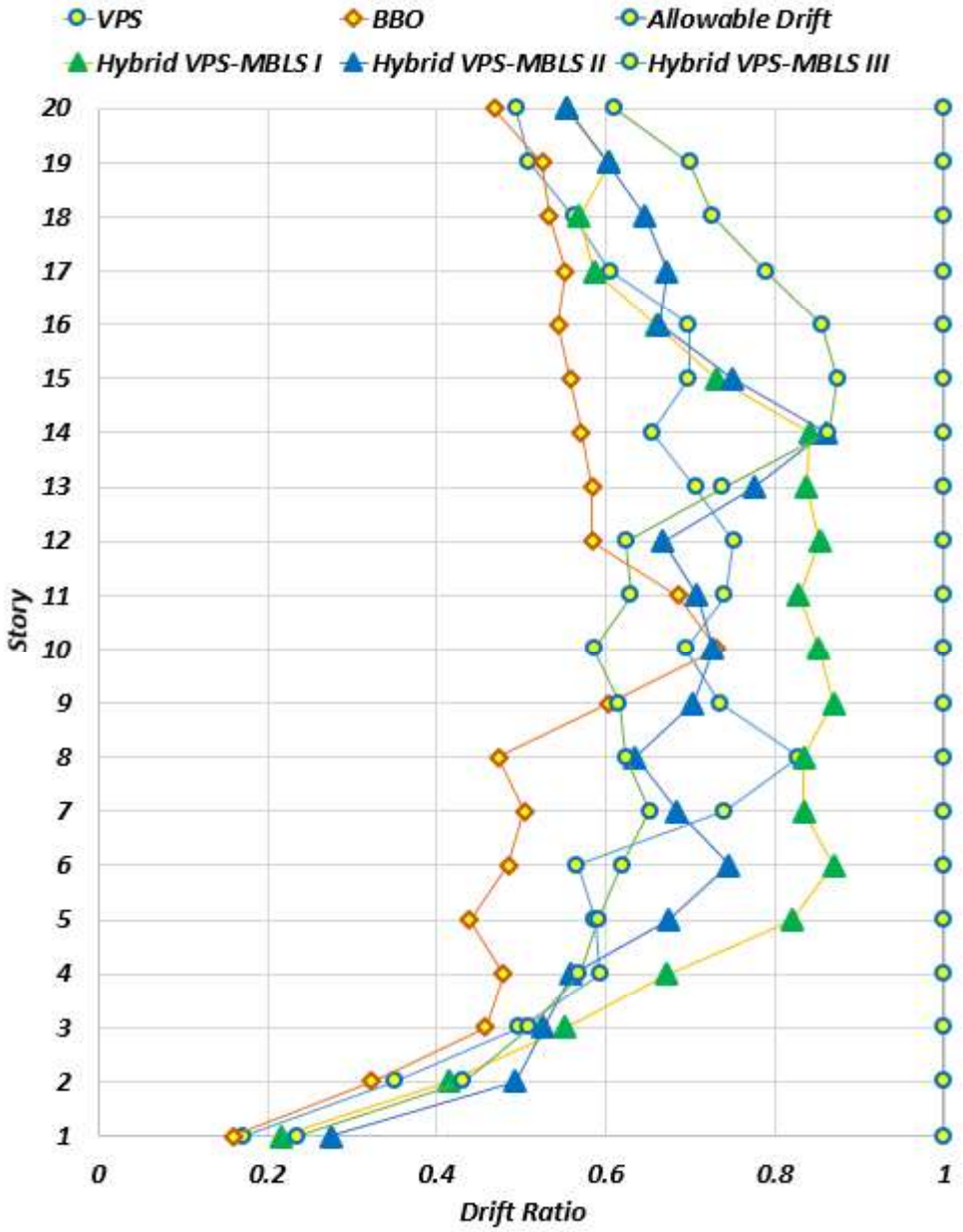

Fig. 23. The drift ratio of the 20-story design example.

7. Concluding Remarks

In this paper, fast and efficient hybrid optimization methods called the VPS-MBLS algorithms are presented for optimum design of steel building structures. In the proposed VPS-MBLS algorithms, the balance between exploration and exploitation is achieved using the VPS as a global optimizer for global exploration and the MBLS as a strong local search mechanism for local exploitation. Based on the type of hybridization, the VPS algorithm and MBLS mechanism are hybridized with parallel, series and mixed series-parallel schemes. These

algorithms effectively use the advantages of both the VPS and MBLS techniques and avoid their weaknesses. In order to investigate performance of the proposed algorithms in attaining optimum designs, three design examples are examined. The obtained results proved that the proposed hybrid methods are capable of providing better results for the considered design examples than the standard metaheuristics. Considering the benchmark 24-story design problem, the third hybrid approaches are capable of providing the best results. The total weight for the 10-story steel structure considering the VPS-MBLS III approach is the best value while the VPS-MBLS I, VPS-MBLS II, VPS and BBO approaches are placed the next places, respectively. The maximum reduction rate is about 8%. The total weight for the 20-story steel structure considering the VPS-MBLS III approach is calculated as 2772.63 ton which is the best value compared to proposed and reported ones. The maximum reduction rate is about 17%. For the optimized structural systems by the VPS-MBLS III approach, stress and drift ratios of the structural elements have higher values and near the allowable value which proves that the provided optimum design sections of the VPS-MBLS III approach have the lowest possible design cross-sections concerning an economic design procedure. In comparison to other optimization techniques in the literature, the numerical results reveal that the VPS-MBLS algorithms are promising approaches capable of obtaining better quality solutions with a less number of required analyses to find optimum design of steel building structures comparing to the other metaheuristic algorithms. For the future challenges, the capability of the proposed hybrid formulations can be investigated by means of other type of problems and compared to other methods.

For the future challenges, the applicability of the proposed hybrid methods can be investigated in dealing with other types of structures such as planar and space trusses. Besides, the considered design examples can also be developed in different perspectives regarding the fact that these buildings can be investigated by means of concrete materials and concrete elements accordingly. It can be mentioned that the applicability of other improvement techniques in enhancing the proposed hybrid algorithms such as upper bound strategy would be a valid choice for the future challenges.

Acknowledgment

This research is supported by a research grant of the University of Tabriz (Number: 1615).

We sincerely express our gratitude to Assoc. Prof. Saeid Kazemzadeh Azad for providing the required data for the design examples.

References

[1] Gallagher RH, Zienkiewicz OC. Optimum structural design: Theory and applications(Book- Optimum structural design: Theory and applications.). London, John Wiley and Sons, Ltd., 1973. 360 p. 1973.

[2] Khot NS, Venkayya V, Berke L. Optimum structural design with stability constraints. International Journal for Numerical Methods in Engineering. 1976;10(5):1097-114.

[3] Jenkins WM. On the application of natural algorithms to structural design optimization. Engineering structures. 1997 Apr 1;19(4):302-8.

[4] Saka MP, Kameshki ES. Optimum design of unbraced rigid frames. Computers & Structures. 1998 Nov 1;69(4):433-42.

[5] Goldberg DE. Genetic algorithms in search, optimization, and machine learning, addison-wesley, reading, ma, 1989. NN Schraudolph and J. 1989;3(1).

[6] Pezeshk S, Camp CV, Chen D. Design of nonlinear framed structures using genetic optimization. Journal of structural engineering. 2000 Mar;126(3):382-8.

[7] Camp C, Pezeshk S, Cao G. Optimized design of two-dimensional structures using a genetic algorithm. Journal of structural engineering. 1998 May;124(5):551-9.

[8] Degertekin SO. Optimum design of steel frames using harmony search algorithm. Structural and multidisciplinary optimization. 2008 Oct 1;36(4):393-401.

[9] Geem ZW, Kim JH, Loganathan GV. A new heuristic optimization algorithm: harmony search. simulation. 2001 Feb;76(2):60-8.

[10] Camp CV, Bichon BJ, Stovall SP. Design of steel frames using ant colony optimization. Journal of Structural Engineering. 2005 Mar;131(3):369-79.

[11] Colorni A, Dorigo M, Maniezzo V. An Investigation of some Properties of an" Ant Algorithm". InPpsn 1992 Sep 28 (Vol. 92, No. 1992).

[12] Atashpaz-Gargari EL, Lucas C. C. 2007. Imperialist Competitive Algorithm: An algorithm for optimization inspired by imperialistic competition. InIEEE Congress on Evolutionary Computation (pp. 4661-4667).

[13] Kaveh A, Talatahari S. Optimum design of skeletal structures using imperialist competitive algorithm. Computers & structures. 2010 Nov 1;88(21-22):1220-9.

[14] Yang XS. A new metaheuristic bat-inspired algorithm. InNature inspired cooperative strategies for optimization (NICSO 2010) 2010 (pp. 65-74). Springer, Berlin, Heidelberg.

[15] Hasançebi OĞ, Carbas S. Bat inspired algorithm for discrete size optimization of steel frames. Advances in Engineering Software. 2014 Jan 1;67:173-85.

[16] Hasançebi OĞ, Azad SK. An exponential big bang-big crunch algorithm for discrete design optimization of steel frames. Computers & structures. 2012 Nov 1;110:167-79.

[17] Murren P, Khandelwal K. Design-driven harmony search (DDHS) in steel frame optimization. Engineering structures. 2014 Feb 1;59:798-808.

[18] Maheri MR, Narimani MM. An enhanced harmony search algorithm for optimum design of side sway steel frames. Computers & Structures. 2014 May 1;136:78-89.

[19] Talatahari S, Azizi M, Optimization of Constrained Mathematical and Engineering Design Problems Using Chaos Game Optimization. Computers & Industrial Engineering. 2020 May 20:106560. https://doi.org/10.1016/j.cie.2020.106560

[20] Azizi M. Atomic orbital search: A novel metaheuristic algorithm. Applied Mathematical Modelling. 2021 May 1;93:657-83. https://doi.org/10.1016/j.apm.2020.12.021

[21] Talatahari S, Azizi M, Optimum design of building structures using Tribe-Interior Search Algorithm. Structures 2020:28:1616-1633. https://doi.org/10.1016/j.istruc.2020.09.075

[22] Talatahari S, Azizi M. Optimal design of real- size building structures using quantum-behaved developed swarm optimizer. The Structural Design of Tall and Special Buildings. 2020 Apr 15:e1747.

[23] Azad SK, Hasançebi O. Upper bound strategy for metaheuristic based design optimization of steel frames. Advances in Engineering Software. 2013 Mar 1;57:19-32.

[24] Kazemzadeh Azad S, Hasançebi O. Computationally efficient optimum design of large scale steel frames. Iran University of Science & Technology, 2014 Jun 10;4(2):233-59.

[25] Azad SK. Design optimization of real-size steel frames using monitored convergence curve. Structural and Multidisciplinary Optimization. 2020 Aug 11:1-22.

[26] Kaveh A, Ghazaan MI. A new meta-heuristic algorithm: vibrating particles system. Scientia Iranica. Transaction A, Civil Engineering. 2017 Apr 1;24(2):551.

[27] Simon D. Biogeography-based optimization. IEEE transactions on evolutionary computation. 2008 Mar 21;12(6):702-13.

[28] AISC Committee. Specification for structural steel buildings (ANSI/AISC 360-10). American Institute of Steel Construction, Chicago-Illinois. 2010.

[29] Jiang Z, Lin Q, Shi K, Pan W. A novel PGSA–PSO hybrid algorithm for structural optimization. Engineering Computations. 2019 Jul 29.

[30] Khalilpourazari S, Khalilpourazary S. An efficient hybrid algorithm based on Water Cycle and Moth-Flame Optimization algorithms for solving numerical and constrained engineering optimization problems. Soft Computing. 2019 Mar;23(5):1699-722.

[31] Yıldız BS, Yıldız AR. The Harris hawks optimization algorithm, salp swarm algorithm, grasshopper optimization algorithm and dragonfly algorithm for structural design optimization of vehicle components. Materials Testing. 2019 Aug 1;61(8):744-8.

[32] Plevris V, Papadrakakis M. A hybrid particle swarm—gradient algorithm for global structural optimization. Computer- Aided Civil and Infrastructure Engineering. 2011 Jan;26(1):48-68.

[33] Kaveh A, Talatahari S. Hybrid algorithm of harmony search, particle swarm and ant colony for structural design optimization. InHarmony search algorithms for structural design optimization 2009 (pp. 159-198). Springer, Berlin, Heidelberg.

[34] Shahin J, and Talatahari S. "Optimum design of truss structures under frequency constraints using hybrid CSS-MBLS algorithm." KSCE Journal of Civil Engineering 22.5 (2018): 1840-1853.

[35] Jalili, Shahin, and Yousef Hosseinzadeh. "Combining migration and differential evolution strategies for optimum design of truss structures with dynamic constraints." Iranian Journal of Science and Technology, Transactions of Civil Engineering 43.1 (2019): 289-312.

[36] Ficarella E, Lamberti L, Degertekin SO. Comparison of three novel hybrid metaheuristic algorithms for structural optimization problems. Computers & Structures. 2021 Feb 1;244:106395.

[37] Aremu A, Ashcroft I, Wildman R, Hague R, Tuck C, Brackett D. A hybrid algorithm for topology optimization of additive manufactured structures. In22nd Annual International Solid Freeform Fabrication Symposium 2011 (pp. 279-289).

[38] Fawaz Z, Xu YG, Behdinan K. Hybrid evolutionary algorithm and application to structural optimization. Structural and Multidisciplinary Optimization. 2005 Sep 1;30(3):219-26.[39] McGuire W. Steel structures. Prentice-Hall. 1968.

[40] MacArthur R, Wilson E. The Theory of Biogeography. Princeton: Princeton University Press. 1967.

[41] ASCE A. Minimum design loads for buildings and other structures. 2010.

[42] Talatahari S, Gandomi AH, Yang XS, Deb S. Optimum design of frame structures using the eagle strategy with differential evolution. Engineering Structures. 2015 May 15;91:16-25.

[43] Azizi M, Ghasemi SA, Ejlali RG, Talatahari S. Optimum design of fuzzy controller using hybrid ant lion optimizer and Jaya algorithm. Artificial Intelligence Review. 2020 Mar;53(3):1553-84.

[44] Kaveh A, Rahmani P, Eslamlou AD. An efficient hybrid approach based on Harris Hawks optimization and imperialist competitive algorithm for structural optimization. Engineering with Computers. 2021 Feb 3:1-29.

[45] Kaveh, A. A comparative study for the optimal design of steel structures using CSS and ACSS algorithms. International Journal of Optimization in Civil Engineering. 2020.